2015

# Understanding Impurities in copper electrometallurgy

Paul Laforest

# UNDERSTANDING IMPURITIES IN COPPER ELECTROMETALLURGICAL PROCESSES

By

PAUL LAFOREST

A THESIS

Presented to the Faculty of the Graduate School of the

MISSOURI UNIVERSITY OF SCIENCE AND TECHNOLOGY

In Partial Fulfillment of the Requirements for the Degree

MASTER OF SCIENCE IN METALLURGICAL ENGINEERING

2015

Approved by

Michael S. Moats, Advisor
F. Scott Miller
Matthew J. O'Keefe

## PUBLICATION THESIS OPTION

Paper I (14-25) in this thesis was prepared in a format to be submitted to Hydroprocess 2015. Paper II (26-46) was prepared in a format to be submitted to Copper 2016.

## ABSTRACT

This work involves examining two industrial reports of methods to handle impurities in copper electrowinning and electrorefining. The first part evaluates the addition of Hydrostar, Cyquest N-900, DXG-F7, and Guartec EW to copper electrowinning electrolyte to affect $MnO_2$ deposition on coated titanium anodes (CTAs). The second part examines the effects of anode chemistry and thiourea addition on the ductility of electrorefined copper starter sheet.

In part one, a laboratory cell was used to simulate a short cycle electrowinning cell via chronopotentiometric operation with an $IrO_2$-$Ta_2O_5$ CTA at 40°C. A cyclic voltammetric sweep was applied after chronopotentiometry to remove any species which had formed on the CTA. The amount of MnO2 removed was quantified by simple application of Faraday's law to the reduction curve. The presence and increase of Mn was confirmed using SEM/EDS. Cyquest N-900 was the only smoothing agent that had a statistically observable effect on $MnO_2$ deposition. Cyquest N-900 demonstrably reduced the amount of $MnO_2$ present on the cathode surface confirming industrial reports.

In part two, another laboratory cell was constructed to simulate industrial conditions during copper electrorefining. Anode material, stripper cell electrolyte, and titanium cathode material were provided by an industrial sponsor. The cell was run continuously for two-week intervals. 21 hour copper deposits produced with a higher As/(Sb+Bi) molar ratio anode were shown to be significantly more ductile than those produced with a lower As/(Sb+Bi) molar ratio anode. The addition of thiourea to a third experimental series, using lower molar ratio anodes, showed that the additive increased the ductility of the cathode to an intermediate value.

# ACKNOWLEDGEMENTS

Thanks are extended to Dr. Michael Moats for continuing patience, learning opportunities, and encouraging demeanor during my course of study. If the quality of graduate education is correlated with one's advisor, mine must be in the top percentiles.

Thanks are also due to my advisory committee members, Dr. Matt O'Keefe and Dr. Scott Miller for their sincerity, graciousness, and willing attitudes.

I am grateful to Dr. Eric Bohannan, for his patience in this work, and to Nathan Inskip, Jack Jones, Nicole Sikes, Teneke Hill, and Denise Eddings for their willingness to help whenever applicable.

I must also extend thanks to Dr. Alex Luyima for being such an excellent conversational partner while working in the lab.

Finally, to my parents, Dennis and Jan Laforest, without whose dogged persistence in life, my existence would not be possible.

# TABLE OF CONTENTS

SECTION

# LIST OF FIGURES

Page

# LIST OF TABLES

Page

# 1. INTRODUCTION

An electrometallurgical process is the final step in refined copper production regardless of ore type. The particular electrometallurgical process used depends on the ore type being treated. Electrowinning (EW) is used to refine material produced by hydrometallurgy, or the leaching of ore, most often by sulfuric acid for copper oxide and some secondary sulfide ores. Electrorefining (ER) is applied to the refinement of acid-refractory primary copper sulfide ores processed by pyrometallurgical methods prior to coming to the tankhouse. It is estimated that 20-25% of the world's refined copper is electrowon from solution produced after leaching copper ores; while 75-80% is produced by electrorefining methods due to the prevalence of primary copper sulfide ores [1, 2].

Copper electrowinning produces about 99.99% pure copper sheet during a week-long plating cycle using 316L stainless steel cathode blanks. This product is stripped from the stainless steel via mechanical means, washed free of acid, and sold at market or used internally to produce copper rod.

A number of organic smoothing agents have been introduced to the copper electrowinning market to replace guar, such as Guartec ®EW, which long been used in industry. Polyacrylamides and polysaccharides, such as Cyquest N-900, Hydrostar ®, and DXG-F7, have been stated to produce smoothing of the cathode deposit and are used commercially [3-7]. Polyacrylamide is also reported to reduce the amount of manganese species deposited on anodes during electrowinning.[7] Due to this latter observation, work (Paper I) was undertaken to attempt to quantify the effect of common commercial additives on the deposition of manganese species on coated titanium anodes in copper electrowinning.

Copper electrorefining occurs after the pyrometallurical processing of ores not amenable to acid leaching. The process produces high purity copper either by plating on a re-usable stainless cathode or a copper starter sheet. Copper starter sheets are produced during a 21-hour plating cycle, using titanium sheet cathodes, which are likewise stripped. The thin deposits are attached to loops produced from other starter sheets and hung in a commercial cell to produce a thick copper deposit.

Anode chemistry in electrorefining is controlled to a certain extent during upstream pyrometallurgical processing. Unfortunately some deleterious elements, such as antimony, still report to the anodes. The inclusion of antimony in the anode results in their presence and buildup in the electrolyte, with can have negative effects on cathode quality [8-14]. Research (Paper II) was conducted to examine the effect of two operating parameters on starter sheet ductility and antimony deportment in the electrolyte.

## 1.1 OBJECTIVES

This thesis is aimed at improving the understanding of impurities present in copper electrometallurgy, both winning and refining. In the first paper, the effects of various commercial smoothing agents, such as Cyquest N-900, Hydrostar, DXG-F7, and Guartec EW on the deposition of manganese as $MnO_2$ on the surface of an $IrO_2$-$Ta_2O_5$ coated titanium anode (CTA) during copper electrowinning were examined. In the second paper, the effects of anode chemistry and thiourea addition on antimony deportment and the ductility of copper starter sheet produced in a laboratory setting were evaluating.

## 1.2 PAPERS

The two papers included in this thesis have been formatted for acceptance at two international conferences on copper processing. Paper I – "Manganese dioxide deposition on catalytic titanium anodes – effect of smoothing agents" was submitted, accepted and presented at Hydroprocess 2015 in Antofagasto, Chile on July 23, 2015. Paper II – "The Effects of Anode Composition and Thiourea on Electrorefined Starter Sheet Ductility and Electrolyte Composition" has been submitted as an abstract to Copper 2016 and is expected to be presented in November 2016 in Kobe, Japan.

Prior to presenting the two papers, an overview of copper processing is given to familiarize the reader with the role and placement of each of the above applications and problems associated.

# 2. LITERATURE REVIEW

## 2.1 ORE TYPES AND PROCESSING

To understand the problems encountered with impurities in copper electrometallurgy, it is advantageous to comprehend the entirety of each process from ore to finished product. The deportment of manganese, antimony, and arsenic throughout the pyro- and hydrometallurgical processes can be important to understanding their chemical forms and interactions during electrowinning and refining.

The mineralogy of ores determine how they will be processed to economically extract the desired pay metal. Broadly, copper ores are separated into oxides, secondary sulfides and primary sulfides. Figure 2.1 shows a general process flow sheet for hydrometallurgical processing from ore to cathode production. Oxide and some secondary sulfide ores are leached and copper is solubilized in the pregnant leach solution (PLS). Copper is concentrated and purified by solvent extraction (SX). Finally, copper is recovered by electrowinning as > 99.99% pure cathode. The hydrometallurgical process reuses the barren products in each step, elegantly reducing acid and organic consumption.

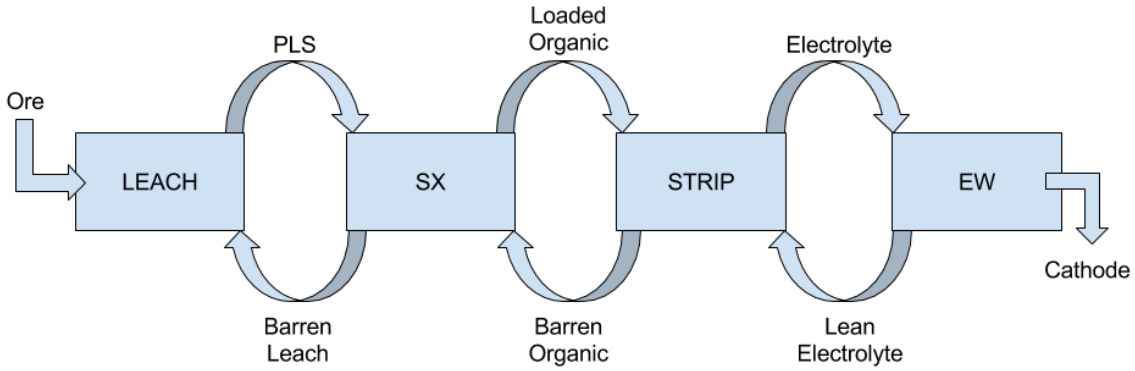


**Figure 2.1:** Basic copper hydrometallurgical processing flow diagram

Primary sulfide and secondary sulfides rich in precious metals are usually recovered using flotation and then treated pyrometallurgically prior to copper recovery by electrorefining. A very basic outline of the process is shown in Figure 2.2. Flotation

chemicals are used to select copper-bearing minerals to produce a concentrate for smelting. Smelting, converting and fire refining result in cast anodes. These anodes are processed through electrorefining (ER) cell, where they will be refined from about 99% pure copper to > 99.99%.

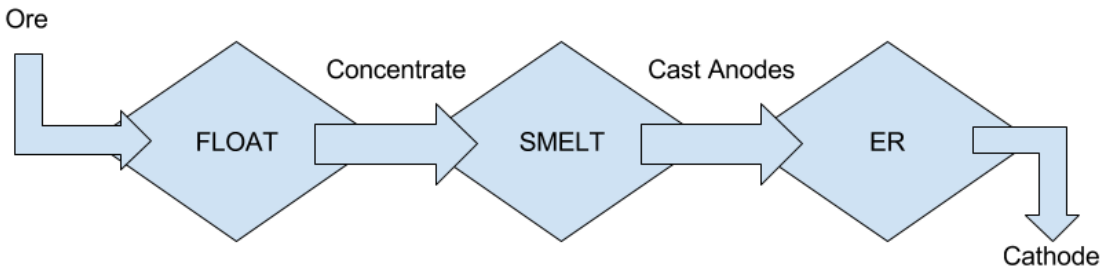


**Figure 2.2:** Basic process diagram of copper pyrometallurgical processing

## 2.2 HYDROMETALLURGICAL PROCESSING

**2.2.1 Leaching.** For copper oxide ores, acid leaching is commonly performed via a process called heap leaching. Appropriately-sized ore is transported to artificially created heaps where it is placed on an impermeable liner and stacked in 'lifts' approximately 5-15 meters high. Some operations include liners between lifts to intercept the leach [15]. The heap is irrigated with a sulfuric acid solution from later in the process that is allowed to percolate through the heap and produce a pregnant leach solution (PLS), which contains the pay metal as well as dissolved impurities, such as $Mn^{2+}$. The PLS is collected in a lined pond. The geometry and stability of the heap plays a large role in how deep each lift can be, the load it can bear, and the flow characteristics of the irrigation solution. The size of the ore affects the density of the heap, becoming the primary factor in geometry and stability considerations. Sizing also affects solution passage through, or permeability of, the heap. Too large a proportion of fine particles may result in the collection of pools of leach solution on the surface or stagnant zones within the heap. Combined with natural precipitation, these may result in solution overflowing from the heap, creating an ecological problem and destabilizing the heap.

Contrarily, if the ore consists mainly of oversized particles, the leach solution may short-circuit, or channel, through the heap, collecting little pay-metal along the way [16,17].

Aside from physical stability, there is the consideration of stability of thermal and acidic conditions within the heap which can be affected by air and water permeability. Leaching of secondary sulfides can be assisted by thermophile bacteria that are usually present in the material. Bacteria such as *Leptospirillum* and *Acidithiobacillus* must be kept at optimal thermal (~30°C) and acidic (0.9-2.5 pH) conditions appropriate for their growth [18]. Under the proper conditions, bacteria generate ferric ions in the ore or irrigated solution and promote the oxidation of sulfide minerals to sulfates, such as in equations (1), (2), and (3), which are dissolved in the leach liquor. Reactions with iron and arsenic bearing minerals also results in the formation of arsenates in the electrolyte. [19]

$$Cu_5FeS_4 + 3O_2 + 6H_2SO_4 \rightarrow 5CuSO_4 + 4S + FeSO_4 + 6H_2O \quad \text{Eq. (1)}$$

$$CuS + 0.5O_2 + H_2SO_4 \rightarrow CuSO_4 + S + H_2O \quad \text{Eq. (2)}$$

$$Cu_2S + O_2 + 2H_2SO_4 \rightarrow 2CuSO_4 + S + 2H_2O \quad \text{Eq. (3)}$$

**2.2.2 Solvent Extraction.** Copper in solution makes its way to the tankhouse from the PLS pond, first passing through mixer-settlers where it undergoes solvent extraction (SX). Because the PLS comes from the ore with a $Cu^{2+}$ content of < 5 g/L, it must undergo further concentration before it can be electrowon. This is accomplished through liquid-liquid separation techniques involving organic phase chemicals that selectively extract $Cu^{2+}$ from the aqueous leach solution. These organic extractants are suspended in an organic solvent, or diluent, such as kerosene, and are in the form of aldoximes or ketoximes, a mixture of which is generally employed that is tailored for a particular operation [19].

The PLS and barren organic phases are combined and agitated to allow for phase interaction. This permits the ionic exchange between the liquids and is performed in a mixer-settler. The phases are allowed to settle and disengage in a large tank, whereupon the loaded organic phase is sent to be stripped. Depending on factors such as ore type and composition, phase ratio, phase contact time, agitation intensity, aqueous pH, and

aqueous content of $Fe^{2+}$, $Mg^{2+}$, $Ca^{2+}$, and silicates, what is called 'crud' may form at the interface of the organic and aqueous phases. This crud results in higher viscosity, longer phase disengagement times, reduced extraction rate, and loss of extractant [20,21].

The loaded organic is stripped using lean electrolyte from the electrowinning process and is sent back to be reused. Iron, manganese, and other elements are not completely eliminated during solvent extraction, some stripping or entrainment causes these impurities to collect in the electrolyte. Indeed, an increase in these impurities can be used as a marker for failing extractants. Most $Mn^{2+}$ is believed to enter the tankhouse by physical entrainment of PLS through the SX process.

**2.2.3 Electrowinning.** Copper is plated from electrolyte using direct electric current. Copper electrowinning is performed at current densities ranging from 150 to 450 $A/m^2$, depending on electrolyte parameters and production needs. While higher current densities are preferred in order to increase overall productivity, the quality and morphology of the deposit can be adversely affected by current densities too high without means of increasing diffusion [22]. Winand [23] diagramed the relationship between plating inhibition and the ratio of cathodic current density (J) to limiting current density ($J_{dl}$), and where common deposit morphologies may be found in experiments with silver nitrate, copper sulfate, and copper and cobalt chloride solutions. In the absence of an organic inhibitor, Winand observed that the intensity of inhibition was related to the exchange current density ($J_0$), where a low $J_0$ correlated to higher inhibition.

**2.2.3.1 Anodes.** Historically, lead anodes are used in copper electrowinning due to lead's abundance, good conductivity, corrosion resistance, and relatively low cost. The corrosion resistance of these anodes is a product of the formation of $PbO_2$ via $PbSO_4$ under oxidative conditions during electrowinning [24-26]. This passivation layer is attributed with the added benefit of self-regeneration in the event of a short circuit between electrodes.

Pb-Ca-Sn and Pb-Sr-Sn anodes were developed to replace Pb-Sb anodes as corrosion issues developed in the cells, and pure lead presented a creep problem at electrowinning temperatures, leading to cracking of the oxide layer and accelerated corrosion [27]. While the dissolution of the anode is reduced by the above alloys, anode corrosion remains a problem and results in short anode lifetimes and Pb contamination of

the copper cathode. To combat these problems, cobalt is generally added to the electrolyte [28-31]. Electrolyte bleed from the tankhouse, necessary to control other impurities, results in the loss of cobalt, constituting a continuous process expense.

The expenses of electricity and cobalt addition, the corrosion of lead anodes, and the contamination of copper cathode material have led to the development of alternative, non-lead anode materials. Principle among these materials has been precious metal oxide-coated titanium, to which a number of tankhouses have been successfully transitioned [32,33]. These coated titanium anodes (CTAs) offer several benefits over common lead anodes. The most important benefit is reduced voltage necessary for electrowinning, which results from the higher activity of the coating. This quality is reported to reduce energy consumption by as much as 15% [34, 35]. Further, because CTAs contain no lead the addition of cobalt to the electrolyte, the cleaning of lead sludge from the cells, and cathode contamination by Pb is eliminated. These benefits are offset by the cost of electrodes and work required to repair anodes damaged by short-circuiting. Because the active coating does not develop in-situ, but is manufactured, it does not possess the self-regenerating quality of the lead oxide layer of lead anodes. Finally, CTAs can be impacted by the deposition of $MnO_2$ from $Mn^{2+}$ in the electrolyte [34].

**2.2.3.2 Manganese.** Problems arising from manganese in the electrowinning electrolyte are known and a number of methods of control have been developed. Reducing manganese concentration in the electrolyte results in increased current efficiency and extended life of solvent extractant (SX) used in the solvent extraction-electrowinning (SXEW) circuit [36,37]. In addition to the common problems of current efficiency and SX lifetime, it has been reported that manganese dioxide forms a passivating layer on the surface of a coated titanium anode, reducing the activity of the coating and mitigating energy savings [31,32,38]. Hence, the work discussed in Paper I which investigates an industry claim that a certain smoothing agent can inhibit or remove $MnO_2$ from CTAs.

## 2.3 PYROMETALLURGICAL PROCESSING

**2.3.1 Flotation.** Sulfide ores that are sufficiently high copper grade, contain significant gold/silver credits, or are acid refractory are treated through an energy-intensive pyrometallurgical process. The ores are crushed and ground before being sent

to flotation cells, where collector chemicals are used to selectively float copper-bearing minerals like chalcopyrite [39]. The collector is a molecule that consists of a chemically active, polar 'head' that selects the target mineral and a hydrophobic, non-polar tail. This hydrophobicity allows attachment to the air bubbles generated by sparging, which carry the attached mineral particles to the surface. Frother chemicals, also are added to stabilize the bubbles produced from sparging, allowing them to remain intact during their ascent to the surface. There are many other factors, including air sparging rate, collector concentration, frother concentration, and ore composition that may affect the efficiency and effectiveness of a flotation operation [40].

Following flotation, the concentrates are thickened, filtered and dried. The concentrate goes on to dewatering via one of several filtration methods. The filter cake is dried at elevated temperature before pyrometallurgical processing [39].

**2.3.2 Smelting/Converting.** Dry concentrate is smelted. Modern flash smelting techniques have improved the efficiency of pyrometallurgical copper refinement over blast furnace or reverbatory furnace techniques by using the exothermic reaction between the sulfides and blown oxygen or oxygen-enriched air to produce copper matte and ferro-silicate slag at around 1150-1250°C [41]. The 40-70% copper matte is transported to a converter, where oxygen is blown through it to remove sulfides, resulting in a further refinement to 98% 'blister' copper and creating more ferrous slag while removing sulfur [40, 42]. The $SO_2$ offgas from smelting and converting is collected and used to produce sulfuric acid for use in leaching and other industrial processes. A reducing gas, such as natural gas, is blown through the copper in an anode furnace to remove excess oxygen, and ~99% pure copper anodes are cast into approximately 1 $m^2$ anodes to be sent to the electrorefining tankhouse.

**2.3.3 Electrorefining.** In contrast to electrowinning, refining utilizes a relatively high purity, cast copper anode which is dissolved during the process. The impurities in the anode material either: (1) report to the electrolyte and remain in solution where they are treated in an electrolyte bleed, (2) report to the electrolyte and precipitate out to the slimes, (3) do not dissolve and remain in the anode slimes, which report to the bottom of the cell, or (4) make their way to the cathode material by electrodeposition or entrainment of slimes. Current density and mass transport in electrorefining are governed

by the same limitations as electrowinning. That is, an optimal current density exists for the formation of compact, high quality cathode deposits, and mass transport through the diffusion layer limits the effect of increasing current density. Copper electrorefining is generally performed at about 65°C, exceeding that of electrowinning to aid in the thermodynamic feasibility of slime formations as well as process kinetics.

**2.3.4 Antimony/Arsenic.** Moats *et al.* [43] examined the deportment of arsenic, bismuth, and antimony, finding that their presence has gradually increased in copper concentrates coming to the smelter for Outokumpu flash smelting and ISASMELT™ processes. From the data presented in Table 1 [43-45], it is evident that much of the arsenic and an appreciable proportion of the antimony present in the concentrate are volatilized during the smelting operations [43].

**Table 2.1**: Deportment of minor elements in flash smelting and ISASMELT™ process

| Element | % to matte | % to slag | % to offgas |
|---|---|---|---|
| Flash Smelting | | | |
| As | 15-40 | 5-25 | 35-80 |
| Pb | 45-80 | 15-20 | 5-40 |
| Zn | 30-50 | 50-60 | 5-15 |
| Bi | 30-75 | 5-30 | 15-65 |
| Sb | 60-70 | 5-35 | 5-25 |
| ISASMELT™ | | | |
| As | 6-10 | 4-8 | 82-90 |
| Pb | 60-65 | 15-20 | 15-25 |
| Zn | 25-30 | 60-70 | 5-10 |
| Bi | 14-25 | 1-2 | 75-85 |
| Sb | 20-40 | 30-40 | 17-45 |

Moats *et al.* further found that the concentration of arsenic in the anode can vary over a wide range up to about 1800 ppm, with an average of about 900 ppm. [46]

In associated work, Moats *et al.* reported a variety of operational As/(Sb + Bi) molar ratios in industry. [47] This ratio is generally maintained at or above 2 to reduce the presence of floating slimes and contamination of the cathode material, but 26% of the reporting facilities were stated to be operating at As/(Sb+Bi) molar ratio less than 2. These elements dissolve from the anode in the trivalent state, becoming oxidized in the

electrolyte during the electrorefining process. The oxidation of Sb(III) to Sb(V) is associated with the formation of amorphous, floating slimes and degradation of cathode quality [8-14]. This work was undertaken to confirm these associations and attempt to mitigate cathode ductility problems associated with an increase in antimony in electrolyte caused by the processing of low molar ratio anodes.

## 2.4 SUMMARY

*In fine*, it has been the goal of the above review to illustrate copper processing methods in order to properly allocate the contained works within the processing streams.

Manganese can have deleterious effects in electrowinning with any anode, as well as causing crud formation and degradation of the liquid-liquid extracting agents. It is generally treated with a solution bleed, but not entirely. Remaining $Mn^{2+}$ can form a passivating layer on coated titanium anodes used to replace common lead anodes.

While antimony in copper electrorefining electrolyte has a negative effect on cathode quality, arsenic can be retained or added to the anode material during smelting to combat antimony by formation of precipitating slimes that report to the bottom of the cell.

## REFERENCES


[1] International Copper Study Group, (2013), The World Copper Factbook 2013, pp. 7.;

[2] M. Moats and M. Free, (2007) "A Bright Future for copper electrowinning", JOM, vol. 59, issue 10, pp. 34-36

[3] C.P. Fabian, (2005) "Copper electrodeposition in the presence of guar or activated polyacrylamide" PhD thesis, James Cook University

[4] C.P. Fabian, M. J. Ridd, and M. E. Sheehan (2007), "Assessment of activated polyacrylamide and guar as organic additives in copper electrodeposition," *Hydrometallurgy*, vol. 86, issue 1, pp. 44-55

[5] S. Sandoval, C. Morales, and C. Bernu, (2010) "Development and Commercialization of Modified Polysaccharide Smoothing Agent for Copper Electrowinning," Preprint 10-113 at SME Annual Meeting, Phoenix, Arizona

[6] https://e-applications.basf-ag.de/data/basf-pcan/pds2/pds2-web.nsf/62007F8EA5718FDEC125757700445004/$File/GUARTEC_r_EW-S1_E.pdf

[7] T.G. Robinson, K.C. Sole, S. Sandoval, A. Siegmund, W.G. Davenport and M. Moats, (2013) "Copper Electrowinning: 2013 World Tankhouse Operating Data," In R. Abel & C. Delgado (Eds.), *Proceeding of Copper 2013 Conference Vol. V Electrowinning/Electrorefining*, pp. 3–14

[8] T.B. Braun, J.R. Rawling, and K.J. Richards (1976) "Factors affecting the quality of electrorefined cathode copper", International Symposium on Copper Extraction & Refining, Las Vegas, Nevada, pp. 511-524

[9] J.P. Demaerel (1987) "The behavior of arsenic in the copper electrorefining process", The Electrorefining and Winning of Copper, Eds. J.E. Hoffmann, R.G. Bautista, V.A. Ettel, V. Kudryk and R.J. Wesely, TMS, Warrendale, PA, U.S.A., 195-210

[10] J.B. Hiskey (2012) "Mechanism and Thermodynamics of Floating Slimes Formation", T.T. Chen Honorary Symposium on Hydrometallurgy, Electrometallurgy and Materials Characterization, pp. 101-112

[11] X. Wang, Q. Chen, Y. Zhou-Lan, and X. Lian-Sheng (2006), "Identification of arsenato antimonates in copper anode slimes", Hydrometallurgy, vol. 84, pp. 211–217

[12] X. Wang, Q. Chen, Y. Zhou-Lan, M. Wang, B. Xiao, and F. Zhang, (2010) "Homogeneous precipitation of As, Sb and Bi impurities in copper electrolyte during electrorefining", Hydrometallurgy, vol. 105, pp. 355-358

[13] X. Wang, Q. Chen, Y. Zhou-Lan, M. Wang, B. Xiao, and F. Tang, (2011) "The role of arsenic in the homogeneous precipitation of As, Sb, and Bi impurities in copper electrolyte", Hydrometallurgy, vol. 108, pp. 199-204

[14] B. Wesstrom (2014) "The Effects of High Antimony in Electrolyte", COM 2014-Conference of Metallurgists Proceedings ISBN:978-1-926872-24-7

[15] R. Thiel and M.E. Smith, (2004) "State of the practice review of heap leach pad design issues", *Geotextiles and Geomembranes*, vol. 22, issue 6, pp. 555-568

[16] G. Jergensen, (1999) "Copper Leaching, Solvent Extraction, and Electrowinning Technology", SME, Inc. 8307 Shaffer Parkway, Littleton, CO, USA 80127, pg. 157

[17] D.W. Kappes, (2002) "Precious metal heap leach design and practice." *Kappes, Cassiday & Associates, Reno, Nevada*.

[18] R. Renman, W. Jiankang, and C. Jinghe, (2006) "Bacterial heap-leaching: Practice in Zijinshan copper mine", *Hydrometallurgy*, vol. 83, issues 1-4, pp. 77-82

[19] D. Dreisinger, (2006) "Copper leaching from primary sulfides: options for biological and chemical extraction of copper", *Hydrometallurgy*, vol. 83, issues 1-4, pp. 10-20

[20] G.A. Kordosky, (1992) "Copper solvent extraction: The state of the art", *JOM*, vol. 44, issue 5, pp. 40-4

[21] L. Jian-she, L. Zhuo-yue, Q. Guan-zhou, and W. Dian-zuo, (2002) "Mechanism of crud formation in copper solvent extraction", *Journal of Central South University of Technology*, vol. 9, issue 3, pp. 169-172

[22] V.A. Ettel, A.S. Gendron, and B.V. Tilak, (1975) "Electrowinning copper at high current densities", *Metallurgical and Materials Transactions B*, vol. 6, issue 1, pp. 31-36

[23] R. Winand, (1991) "Electrocrystallization: fundamental considerations and application to high current density continuous steel sheet plating", *Journal of Applied Electrochemistry*, vol. 21, issue 5, pp. 377-385

[24] I. Ivanov, Y. Stefanov, Z. Noncheva, M. Petrova, TS. Dobrev, L. Mirkova, and R Vermeersch, J.-P Demaerel, (2000) "Insoluble anodes used in hydrometallurgy: Part I. Corrosion resistance of lead and lead alloy anodes", Hydrometallurgy, Volume 57, Issue 2, pp.109-124

[25] I. Ivanov, Y. Stefanov, Z. Noncheva, M. Petrova, TS. Dobrev, L. Mirkova, R Vermeersch, and J.-P Demaerel, (2000) “Insoluble anodes used in hydrometallurgy: Part I. Corrosion resistance of lead and lead alloy anodes”, Hydrometallurgy, Volume 57, Issue 2, 1 September 2000, pp. 125-139

[26] A. Nikoloski, M. Nicol, and A. Stuart. "Managing the passivation layer on lead alloy anodes in copper electrowinning." (2010): *GDMB Copper 2010, Hamburg*, Germany, vol. 4, pp. 1559-1568

[27] A. Felder and R. D. Prengaman, (2006) “Lead alloys for permanent anodes in the nonferrous metals industry”, JOM Vol. 58, Issue 10, pp. 28-31

[28] G. Eggett and D. Naden. "Developments in anodes for pure copper electrowinning from solvent extraction produced electrolytes." *Hydrometallurgy* 1.2 (1975): 123-137.

[29] A. S. Gendron, V. A. Enel, and S. Abe. "Effect of cobalt added to electrolyte on corrosion rate of Pb-Sb anodes in copper electrowinning." *Canadian Metallurgical Quarterly* 14.1 (1975): 59-61.

[30] A. Hrussanova, L. Mirkova, and TS. Dobrev, (2002) “Journal of Applied Electrochemistry 32, pp. 505-512; P. Yu, T. J. O’Keefe, (1999) “Evaluation of Lead Anode Reactions in Acid Sulfate Electrolytes. I. Lead Alloys with Cobalt Additives, *J. Electrochem. Soc.*, vol. 146, issue 4, pp. 1361-1369

[31] A. Nickoloski, and M.J. Nicol, (2008) “Effect of cobalt ions on the performance of lead anodes used for the electrowinning of copper-A literature review”, *Mineral Processing and Extractive Metallurgy Review*, 29(2), pp. 143-172

[32] S. Sandoval, C. Clayton, E. Gebrehiwot, and J. Morgan, (2013), *Tankhouse Parameters for Transition from Lead to Alternative Anodes*, Hydroprocess 2013

[33] S. Sandoval, R. Garcia, T. Neff, and N. Schnebly, (2013), *Operation of Alternative Anodes at Chino SXEW*, Proceedings of Copper 2013, Santiago Chile.

[34] M. Moats, (2010), MnO2 Deposition on Coated Titanium Anodes in Copper Electrowinning Solutions, Erzmetall vol. 63, pp. 286–291

[35] M. Morimitsu, N. Oshiumi, and N. Wada, (2010), “Smart Anodes for Electrochemical Processing of Copper Production”, *GDMB Copper 2010*, Hamburg, Germany, vol. 4, pp. 1511-1519

[36] C.Y. Cheng, C.A. Hughes, K.R. Barnard, and K. Larcombe, (2000) “Manganese in copper solvent extraction and electrowinning”, *Hydrometallurgy*, vol. 58, issue 2, pp. 135-150

[37] W. Zhang and C.Y. Cheng, (2007) "Manganese metallurgy review. Part III: Manganese control in zinc and copper electrolytes", *Hydrometallurgy*, vol. 89, issues 3-4, pp. 178-188

[38] S. Nijjer, J. Thonstad, and G.M. Haarberg, (2001) "Cyclic and linear voltammetry on Ti/$IrO_2$-$Ta_2O_5$-$MnO_x$ electrodes in sulfuric acid containing $Mn^{2+}$ ions", *Electrochimica Acta*, vol. 46, issue 23, pp. 3503-3508

[39] A. K. Biswas and W.G. Davenport, (1980) "Extractive Metallurgy of Copper" 2nd Ed., Pergamon Press Inc, Maxwell House, Fairview Park, Elmsford New York 10523, USA.

[40] V.D. Smar, R.R. Klimpel, and F.F. Aplan, (1994) "Evaluation of chemical and operational variables for the flotation of a copper ore Part I – Collection concentration, frother concentration, and air flow rate", *Int. Journal of Mineral Processing*, vol 42, pp. 225-240

[41] W.G. Davenport and E.H. Partelpoeg, (1987) "Flash Smelting: Analysis, Control, and Optimization", Pergamon Press Inc, Maxwell House, Fairview Park, Elmsford New York 10523, USA

[42] M. Nagamori and P.J. Mackey, (1978), "Thermodynamics of copper matte converting: Part I. Fundamentals of the noranda process", *Met. Trans. B*, vol. 9, issue 2, pp. 255-265

[43] M.S. Moats, N. Aslin, A. Pranowo, R.F. Gerardo, and F. Alvear, (2014) "Arsenic's Behavior and Benefits in Copper Electrorefining", *William Davenport Symposium, COM 2014*

[44] W.G. Davenport, D.M. Jones, M.J. King, and E.H. Partelpoeg, (2001) "Flash Smelting: Analysis, Control and Optimization", *TMS*, Warrendale

[45] C.R. Fountain, M.D. Coulter, and J.S. Edwards, (1991) "Minor Element Distribution in the Copper ISASMELT process", In *C. Diaz, C. Landolt and A. Luraschi (Eds.), Copper 1991,* vol. IV, pp. 359-370, Pergamon Press

[46] M. Moats, T. Robinson, and S. Wang, (2014) "A review of copper electrorefining operating data – 1987 to 2013", *Proceedings of the William Davenport Symposium*. Canadian Institute of Mining, Metallurgy and Petroleum, Montreal, Canada

[47] M. Moats, T. Robinson, S. Wang, A. Filzwieser, A. Siegmund, and W. Davenport, (2013) "Global Survey of Copper Electrorefining Operations and Practices", *Copper 2013*, vol. V, pp. 307-317. The Chilean Institute of Mining Engineers, Chile.

## PAPER

# I. Manganese dioxide deposition on catalytic titanium anodes – effect of smoothing agents

Paul Laforest and Michael Moats

Materials Research Center, Missouri University of Science and Technology, USA

## ABSTRACT

The replacement of lead alloy anodes with catalytic titanium anodes (CTAs) has occurred in several copper electrowinning tankhouses in North and South America. However, the effects of contaminants and additives in the electrolyte on CTAs are still being investigated. Manganese dioxide ($MnO_2$) can form on the surface of CTAs blocking the active surface area and increasing the potential for oxygen evolution, thereby lessening the benefits of catalytic titanium anodes. Therefore, understanding the effects of commercial electrolyte parameters on $MnO_2$ deposition is important in the implementation of these energy saving devices.

An electrochemical technique was developed to evaluate the effect of common impurities and smoothing agents on the deposition of $MnO_2$ on CTAs. The technique involved a two-step experiment. CTAs were operated with constant current in 40°C synthetic copper electrowinning electrolytes for one hour. Then any $MnO_2$ deposited was removed using voltammetry. The voltammetry results were analyzed to quantify the amount of $MnO_2$ deposited.

Using this method, it was found that Cyquest N-900 decreased the amount of $MnO_2$ deposited while HydroStar, DXG-F7 or Guartec EW did not have a statistical effect. In the presence of N-900, increasing iron concentration decreased the amount of $MnO_2$ deposited while increasing cobalt concentration had no effect. The impact of these results on operations is discussed.

**Keywords:** Copper, Electrowinning, Titanium Anode, Alternative Anode, Manganese, Manganese Dioxide, Smoothing Agent, Cyclic Voltammetry

## INTRODUCTION

Approximately 22% of the primary refined copper in the world is produced via electrowinning (EW) (International Copper Study Group, 2013) Copper electrowinning is typically carried out using stainless steel blanks as cathodes and lead alloy sheets as anodes. These anodes are increasingly disadvantageous as heavy metal handling becomes more problematic. Lead corrosion in electrowinning cells is a consistent maintenance issue. As the lead corrodes, flakes slough off, falling to the bottom of the cell, and require periodic cleaning. To reduce corrosion, which leads to sludge formation and Pb contamination of the cathode, many copper electrowinning tankhouses add cobalt ion to the electrolyte. This cobalt is lost when electrolyte is bled from the tankhouse to control other impurities, such as iron, manganese, or chloride. In accordance with the modern drive toward sustainable industry, as well as increasing production efficiency, catalytic titanium anodes (CTAs) have seen an increase in application in copper electrowinning operations. This is due to the initial energy savings of about ~15% versus lead anodes, elimination of cobalt addition for corrosion resistance, and the desire to reduce lead handling in industrial plants (Sandoval *et al 2,* 2013).

Manganese in solution can become problematic when it deposits on the surface of CTAs as an oxide or oxyhydroxide, reducing the life of the anode by as much as 18% (Sandoval *et al 1,* 2013). The manganese species create a passivating layer on the surface, reducing the effective anode area and increasing the current density on the exposed areas. This both reduces the effective life of the precious metal coating and increases the potential necessary to sustain the amperage. The presence of intermediate, high oxidation states of Mn, such as $Mn^{3+}$ and permanganate, has also been correlated with degradation in the effectiveness of common copper solvent extractants, including reduced kinetics and capacity of the organic (Cheng *et al,* 2000; Miller, 2013). Amorphous MnOOH, an intermediate to the formation of $MnO_2$ on PbCaSn anodes, is dependent upon the concentration of $Mn^{3+}$ in the electrolyte, and its formation can be mitigated by the presence of $Fe^{3+}$ as a reductant (Ipinza *et al*, 2007; Nijjer, Tonstad & Haarberg, 2000; Preisler, 1976; Zhang & Cheng 1, 2007; Zhang & Cheng 2, 2007; Chotkowski, Rogulski & Czerwinski, 2011; Rodrigues, Munichandraiah & Shukla, 1998). This mechanism has

been described, with respect to the deposition of electrolytic manganese dioxide (EMD) in sulfuric acid solutions, by the following reactions:

$$2Mn^{2+} \rightarrow 2Mn^{3+} + 2e \quad (1)$$

$$2Mn^{3+} \rightarrow 2Mn^{2+} + Mn^{4+} \quad (2)$$

$$Mn^{4+} + 2H_2O \rightarrow MnO_2 + 4H^+ \quad (3)$$

Commercially, organic additives are used in the copper EW cell to smooth the cathode deposit, ultimately preventing operational problems such as shorts between electrodes from excessive dendritic growth (nodules) and producing superior product. The understood mechanism is that of organic adsorption to the surface at areas of higher current density, blocking those areas to deposition and promoting more uniform reduction of copper onto the cathode.

It has been reported that a polyacrylamide additive also inhibits manganese deposition on CTAs (Sandoval *et al* 1, 2013). This work is intended to examine the effect of the various commercial organic additives on the deposition of manganese on commercial $IrO_2$-$Ta_2O_5$ coated titanium samples.

Iron is also present in electrowinning solutions, and effort is made to maintain the Fe/Mn ratio above a certain level. This has the effect of reducing the amount of $MnO_2$ species deposited (Ipinza *et al*, 2007; Sandoval *et al* 1, 2013). This effect is also studied with respect to the addition of organics and cobalt.

**METHODOLOGY**

The various electrolyte solutions were prepared using 95-98% sulfuric acid (GFS Chemicals), 98-102% $CuSO_4 \cdot 5H_2O$ (GFS Chemicals), ≥ 99% $MnSO_4 \cdot H_2O$ (Sigma-Aldrich), ≥ 98% $CoSO_4 \cdot 7H_2O$ (Sigma-Aldrich), ≥ 97% $FeSO_4 \cdot 5H_2O$ (Fisher Scientific), ≥ 99% NaCl and distilled, deionized, 18.3 MOhm water. Organic additives were prepared by dissolution in water at a concentration of 3.5 g/L and then added to the electrolyte to obtain the targeted concentration. All electrolytes consisted of 180 g/L $H_2SO_4$, 40 g/L Cu, 20 mg/L Cl. Remaining parameters were varied experimentally.

A Gamry Reference 3000 Potentiostat/Galvanostat was used for all electrochemical experiments. A three electrode cell was employed. The working electrode was a coupon of commercially available $IrO_2$-$Ta_2O_5$ coated titanium. The counter electrode was 316L stainless steel plated with copper. The reference electrode was a $Hg/HgSO_4$ – Ag/AgCl, double junction reference electrode at 0.22 V versus SHE. Temperature of the cell was maintained in a water bath at 40 ± 1 °C. A thermometer was inserted into the cell to monitor solution temperature directly. No external agitation of the electrolyte was provided.

An anode sample was prepared by shearing a commercial catalytic titanium sheet with a crystalline non-proprietary $IrO_2$-$Ta_2O_5$ coating to produce a coupon with an apparent surface area of 5.7 $cm^2$. The coating was then removed from one face by grinding. The coupon was then resistance welded to a short (7.6 cm), 0.32 cm diameter grade 2 titanium rod to which the Gamry instrumentation was connected.

The cell was operated using three sequential electrochemical methods. First, cyclic voltammetry (CV) was performed by sweeping the potential from 0.75 to 1.5 V vs. ref. and then returning the potential to 0.75 V at a sweep rate of 1 mV/s. The initial CV was conducted to insure the titanium anode was cleaned from the prior experiment and was operating with typical activity. Then the electrode was operated at constant current density of 435 $A/m^2$ for 60 minutes depositing manganese oxide and evolving oxygen. After the constant current portion, another CV experiment was conducted by sweeping the potential from 1.5 to 0.75 V versus reference, and then back to 1.5 V at a sweep rate of 1 mV/s. The purpose of the second CV was to reduce any manganese oxide that had formed during the previous electrochemical tests. Each condition was replicated at least once.

The charge associated with the reduction of manganese oxide was determined from the area under the zero line, shown in Figure 1. The charge was used to calculate the amount of manganese reduced using Faraday's Law, Eq. 4:

$$m = \frac{Q\ MW}{n\ F} \tag{4}$$

Where $m \equiv$ the mass, in grams, of manganese dioxide dissolved from the anode;
$Q \equiv$ the charge passed during the reduction of Mn;

*MW* ≡ the molecular weight of the reduced specie assumed to be $MnO_2$;

*n* ≡ the number of electrons exchanged – assumed to be two from the overall reaction given in Eq 5;

*F* ≡ Faraday's constant with a value of 96,485 Coulombs/mole of electrons;

$$MnO_{2\,(s)} + 4H^{+} + 2e^{-} \rightarrow Mn^{2+} + 2H_2O, \qquad E^{\circ}=1.230\ V \qquad (5)$$

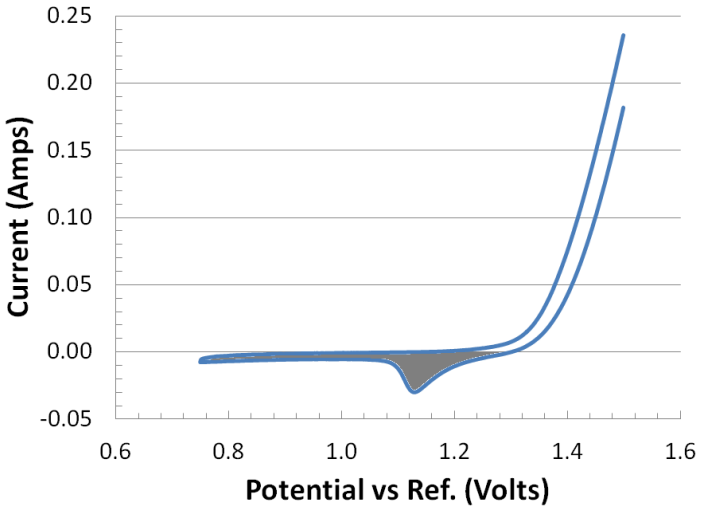


**Figure 1** Example CV of dissolution of $MnO_2$ from the anode surface by the reduction of $MnO_2$ to $Mn^{2+}$. Shaded area was used in the theoretical calculation of $MnO_2$ deposited to ascertain the charge passed

## RESULTS AND DISCUSSIONS

The electrochemical method was first evaluated by examining the effect of increasing manganese concentration in solution. As $MnSO_4$ concentration increased (see Figure 2), the apparent amount of $MnO_2$ deposited, as calculated from Mn, on the surface as measured electrochemically increased. This is in agreement with literature (Bodoardo *et al*, 1994). The presence of manganese on the anode surface after the one hour constant current portion of the test was also examined using energy dispersive spectroscopy (EDS). The EDS intensity associated with the Mn K-alpha energy peak increased with increasing manganese in solution and correlated with the reduction charge measured by

the electrochemical method. This indicated that the electrochemical method was measuring the reduction of the manganese oxide from the anode surface.

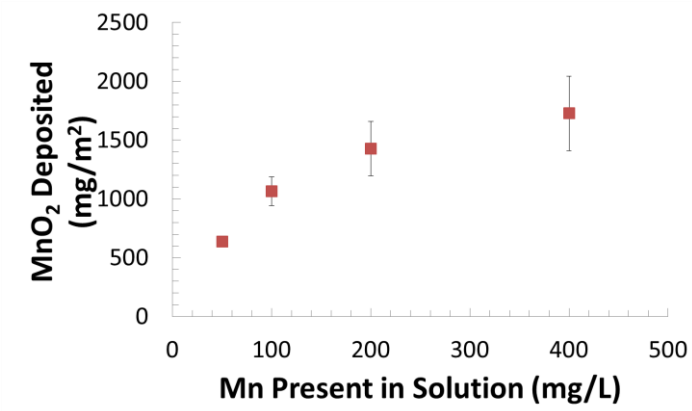


**Figure 2** Amount of deposited manganese oxide as Mn concentration in synthetic copper electrowinning electrolyte is increased

**Effect of Smoothing Agents**

The effect of common copper electrowinning cathode smoothing agents (DXG-F7, HydroStar, Guartec EW and Cyquest N-900) on the amount of manganese oxide deposited on CTAs during the initial CV and one hour constant current density experiment was examined. All experiments were conducted using 8 mg/L of organic additive in a synthetic solution of 180 g/L $H_2SO_4$, 40 g/L Cu, 200 mg/L Mn, 200 mg/L Co, 20 mg/L $Cl^-$, 2 mg/L Fe at 40$^o$C. The results are presented in Figure 3.

The data indicate significant variation in the amount of manganese deposited on the CTAs in the absence of smoothing agents. While the average $MnO_2$ deposited increased with the addition of DXG-F7, HydroStar, or Guartec EW to the solution, the difference was not greater than the variation observed in the absence of these additives. Therefore, it is concluded that these additives do not have a statistically significant effect on the amount of $MnO_2$ deposited on the CTA.

Even with the variation noted, the effect of adding Cyquest N-900 is obvious. The addition of 8 mg/L of Cyquest N-900 decreased the average $MnO_2$ deposited from 0.69 g/m$^2$ to 0.25 g/m$^2$, which represents a 64% decrease. The addition of N-900 also decreased the variation in the amount of Mn deposited as an oxide. Obviously, N-900

has a strong positive effect on inhibiting the deposition of manganese oxide on CTAs confirming the earlier industry report (Sandoval *et al 1*,2013)

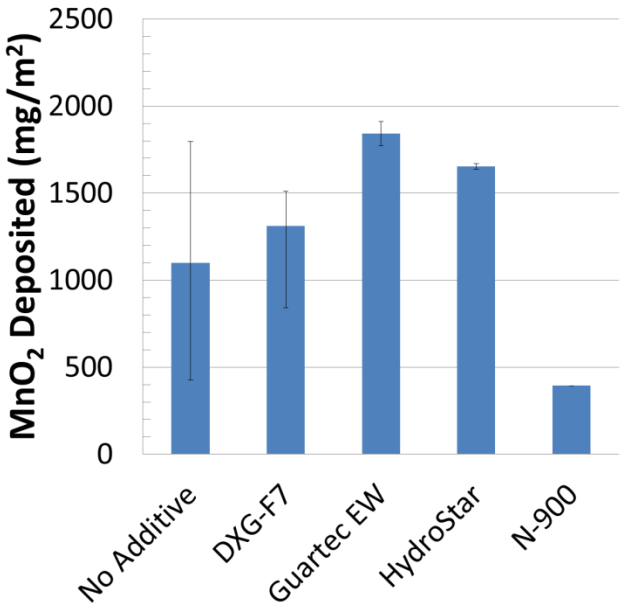


**Figure 3** Organic effects at 8 mg /L on the amount of Mn deposited on the anode surface during a 60 minute test at 435 A/m2 in 180 g/L $H_2SO_4$, 40 g/L Cu, 200 mg/L Mn, 200 mg/L Co, 20 mg/L $Cl^-$, 2 mg/L Fe

N-900 is a polyacrylamide which has an N-bearing amide group. The other additives examined are polysaccharide based compounds, which do not contain this functionality. How this functional group is affecting the deposition of $MnO_2$ is unclear. No differences were observed in the potential during the constant current experiments or at which the reduction of $MnO_2$ occurred in the CV scans.

For $MnO_2$ to deposit on the anode, Mn (II) must oxidize to create an aqueous $Mn^{3+}$ intermediate species, which further oxidizes to $MnO_2$. The $Mn^{3+}$ species may be reduced by N-900. This would prevent the formation of $MnO_2$. Further study is needed to determine if N-900 reduces $Mn^{3+}$ to $Mn^{2+}$ and if other N-bearing compounds have similar effects.

### *Effect of N-900 Concentration*

The effect of the concentration of Cyquest N-900 on the formation of manganese oxide was examined. Results are shown in Figure 4. This data was collected in the absence of iron addition to the electrolyte. It appears the concentration of N-900 needs to be great enough (e.g. greater than 1 mg/L) to achieve a noticeable decrease in the manganese oxide deposition. Under the conditions of this test, increasing N-900 concentration above 8 mg/L did not further decrease the deposition of manganese oxide. These effects should be examined using longer term experiments.

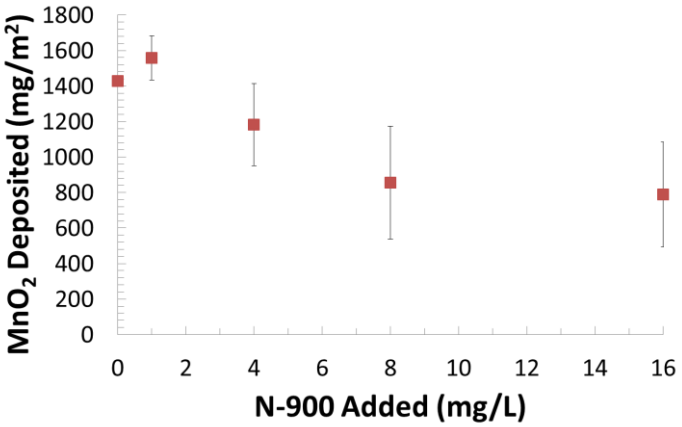


**Figure 4** The effect of N-900 concentration on the amount of Mn deposited on the anode surface during a 60 minute test at 435 A/m2 in 180 g/L $H_2SO_4$, 40 g/L Cu, 200 mg/L Mn, 20 mg/L $Cl^-$; no Fe added

### *Iron Effect*

It is known that an interaction between manganese oxidation and the presence of iron in solution exists (Pilla, Duarte & Mayer, 2004). Thus, the interaction between iron and manganese in the presence of N-900 was examined. Low concentrations of Fe(III) were added to the solution to observe its effect on manganese oxide deposition. As Fe(III) concentration increased even in the mg/L range, there was reduction in the amount of Mn deposited, but this plateaued above about 2 mg/L Fe. An addition set of experiments was performed using 1000 mg/L Fe(III), as this concentration is more commercially relevant. These experiments produced no significant change in the amount

of manganese oxide deposited when compared the results at 2-6 mg/L Fe(III). Figure 5 shows the average of two runs of each experimental condition, omitting those performed at 1000 mg/L.

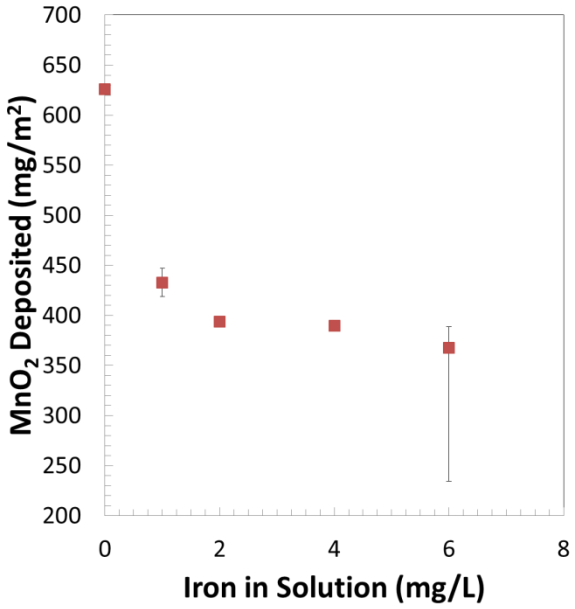


**Figure 5** Fe(III) added to solution decreases the amount of Mn deposited. 180 g/L $H_2SO_4$, 40 g/L Cu, 200 mg/L Mn, 200 mg/L Co, 20 mg/L $Cl^-$, 8 mg/L N-900

### *Cobalt Effect*

Previous research has indicated that an interaction between manganese and cobalt concentration on the amount on $MnO_2$ deposited on CTAs might exist (Moats, 2010). The existence of this possible interaction was examined in the presence of N-900. Cobalt was added as $CoSO_4$ at concentrations of 50, 100, or 400 mg/L. The addition of cobalt did not appear to have an effect on the amount of $MnO_2$ deposited on the anode in the presence of N-900 and a little iron, as seen in Figure 6.

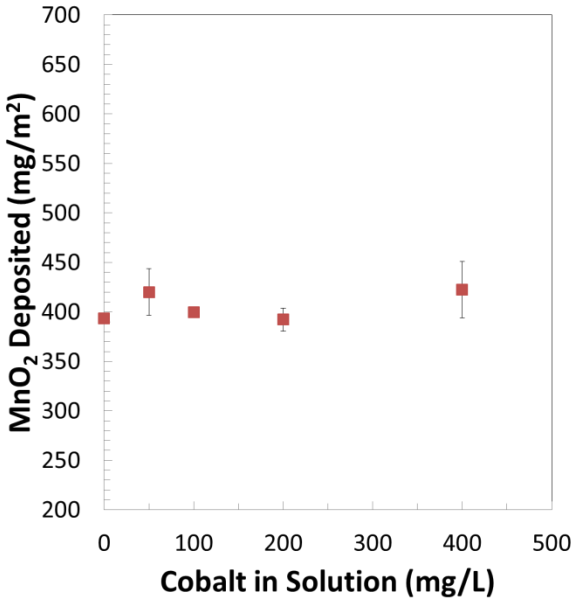


**Figure 6** Effect of cobalt concentration on $MnO_2$ deposition. 180 g/L $H_2SO_4$, 40 g/L Cu, 200 mg/L Mn, 20 mg/L $Cl^-$, 2 mg/L Fe, 8 mg/L N-900

***Industrial Relevance***

This work was conducted to confirm previous industrial reports that N-900 inhibited the formation of $MnO_2$ on CTAs. This electrochemical study confirmed this observation under controlled laboratory conditions.

A few items should be noted in applying these results to industrial tankhouses. First, all work in this study was performed using a crystalline $IrO_2$ coating. This coating is not believed to be the same as those employed in catalytic titanium anodes that have been installed and/or demonstrated in copper electrowinning facilities. However, the ability of N-900 to inhibit $MnO_2$ formation on these anodes is believed to be transferrable. When titanium anodes are evaluated, the formation of $MnO_2$ on the surface of the anodes should be monitored.

It has also been reported that N-900 can destabilize lead anode scale by removing $MnO_2$ from the surface. This has resulted in upsets and decreased cathode purity (Sandoval *et al* 1, 2013). Therefore, the addition of N-900 to mitigate $MnO_2$ formation on titanium anodes should occur after conversion to titanium anodes or with great caution.

## 3. CONCLUSIONS

In this study, the ability of Cyquest N-900 to inhibit $MnO_2$ deposition on catalytic titanium anodes was confirmed by an electrochemical method in controlled laboratory testing. Polysaccharide based smoothing agents like HydroStar, DXG-F7 and Guartec EW did not inhibit $MnO_2$ deposition. Small concentrations (2-6 mg/L) of Fe(III) further reduced $MnO_2$ deposition in the presence of 8 mg/L N-900. The presence of cobalt in solution did not affect $MnO_2$ deposition in the presence of N-900.

## REFERENCES

Bodoardo S., Brenet J., Maja M., Spinelli P., (1994), *Electrochemical Behaviour of $MnO_2$ Electrodes in Sulphuric Acid Solutions*, Electrochimica Acta vol. 39 (13), pp. 1999–2004.

Cheng C.Y., Hughes C.A., Bernard K.R., Larcombe K., (2000), *Manganese in copper solvent extraction and electrowinning*, Hydrometallurgy vol. 58, pp. 135–150.

Chotkowski M., Rogulski Z., Czerwinski A., (2011), *Spectroelectrochemical investigation of $MnO_2$ electro-generation and electro-reduction in acidic media*, Journal of Electroanalytical Chemistry vol. 651, pp. 237–242.

International Copper Study Group, (2013), *The World Copper Factbook 2013*, pp. 7.

Ipinza J., Ibanez J. P., Pagliero A., Vergara F., (2007), *Mechanismo de la formacion de compuestos de manganese en electrolitos acidos*, Revista de Metalurgia vol. 43 (1), pp. 11–19.

Mella S., Villarroel R., Lillo A., (2004), *Copper Electrowinning in the Absence of Acid Mist: Six Years of Industrial Application*, Ingenieria Industrial Same LTDA, Chile

Miller G., *Recent Experience with Manganese and its Effects on Copper SX-EW Operations*, Miller Metallurgical Services.

Moats, M., (2010), *$MnO_2$ Deposition on Coated Titanium Anodes in Copper Electrowinning Solutions*, Erzmetall vol. 63, pp. 286–291.

Nijjer S., Thonstad J., Haarberg G. M. (2000), *Oxidation of Manganese(II) and Reduction of Manganese Dioxide in Sulphuric Acid*, Electrochimica Acta vol. 46, pp. 395–399.

Pilla A., Duarte M., Mayer C., (2004), *Manganese dioxide electrodeposition in sulphate electrolytes: the influence of ferrous ions*, Journal of Electroanalytical Chemistry vol. 569, pp. 7–14.

Preisler E., (1976), *Electrodeposited Manganese Dioxide with Preferred Crystal Growth*, Journal of Applied Electrochemistry vol. 6, pp. 301–310.

Rodrigues S., Munichandraiah N., Shukla, A., (1998), *A cyclic voltammetric study of the kinetics and mechanism of electrodeposition of manganese dioxide*, Journal of Applied Electrochemistry vol 28, pp. 1235–1241.

Sandoval S., Clayton C., Gebrehiwot E., Morgan J., (2013), *Tankhouse Parameters for Transition from Lead to Alternative Anodes*, Hydroprocess 2013.

Sandoval S., Garcia R., Neff T., and Schnebly N., (2013), *Operation of Alternative Anodes at Chino SXEW*, Proceedings of Copper 2013, Santiago Chile.

Zhang W., Cheng C. Y., (2007), *Manganese Metallurgy Review. Part II: Manganese Separation and Recovery from Solution*, Hydrometallurgy vol. 89, pp. 160–177.

Zhang W., Cheng C. Y., (2007), *Manganese Metallurgy Review. Part III: Manganese Control in Zinc and Copper Electrolytes*, Hydrometallurgy vol. 89, pp. 178–188.

## II. The Effects of Anode Composition and Thiourea on Electrorefined Starter Sheet Ductility and Electrolyte Composition

Paul Laforest and Michael Moats


### ABSTRACT

Antimony in smelted copper anodes has been shown to cause problems in electrorefining including brittleness of starter sheets. In order to improve deposit properties, a two part study was conducted examining the effect of anode chemistry and thiourea addition on electrolyte chemistry and cathode ductility. In the first part, two anodes with different molar ratios of As/(Sb+Bi) were used in laboratory electrorefining experiments with commercial electrolyte, and the addition of commercial glue and Avitone. In the second part, thiourea was added to the system to examine its effect while using the lower molar ratio anode. The ductility of 21-hr copper deposits was evaluated by a 180° bend test. X-ray diffraction (XRD) and metallography were performed on unbent specimens to characterize the deposit structure. The 3.8 molar ratio anode resulted in an increase, on average, from four to eight bends to failure in cathode material, improving over the 0.54 molar ratio anode. Cathode produced in the presence of thiourea resulted in a higher average number of bends to failure (six) than cathode material produced without thiourea (four). Significantly lower concentration of antimony (V) was detected when operating with higher molar ratio anode. Thiourea also reduced the concentration of Sb (V) in the electrolyte. XRD data shows all deposits to be predominately (220) crystallographic orientation. The presence of (111) and (200) planes was noted in cathode material produced from the higher molar ratio anode suggesting that mixed growth character could be responsible for the observed increase in bend test results. These planes also appeared in the cathode produced in the presence of thiourea with lower molar ratio anode, although in lesser proportion than using higher molar ratio anode alone. In summary, the ductility of the starter sheet materials was improved by a higher anode molar ratio or the addition of thiourea


### INTRODUCTION

The presence of antimony in copper electrorefining electrolyte has been reported to cause problems in cathode production (Hiskey, 2012; Peng, Zheng & Chen, 2012; Wang *et al.*, 2006; Wang *et al.*, 2010; Wang *et al.*, 2011; Wesstrom, 2014). To better

understand the impact of antimony, laboratory scale electrorefining experiments were conducted using industrial inputs (anodes, cathodes and electrolyte). The influences of anode chemistry or thiourea addition on the valences of antimony and arsenic in the electrolyte were monitored and correlated to physical cathode characteristics, such as a bend test to failure and crystallographic orientation.

Commercially, starter sheets are produced by electrorefining impure cast copper anodes onto titanium blanks. The starter sheets are then hung in an electrorefining or electrowinning cell using loops of bent starter sheet material. These loops, in the absence of sufficient ductility, fail, resulting in cathodes falling into the electrolysis cells. It is thought that the reduction in ductility is related to anode composition; in particular, the molar ratio of arsenic to antimony plus bismuth (As/Sb+Bi). It has been stated that maintaining this ratio above 2:1 results in numerous improvements to electrorefining operations (Baltazar, Claessens & Thiriar, 1987; Kamath *et al.*, 2003; Krusmark, Young & Faro, 1995; Noguchi, Itoh & Nakamura, 1995; Wenzl, 2008).

Historically, maintaining the proper As/(Sb+Bi) ratio has been addressed by the addition of arsenic at the smelter. Arsenic in the anode dissolves into solution during electrorefining as $As^{3+}$ and then oxidizes from $As^{3+}$ to $As^{5+}$ prior to the oxidation of $Sb^{3+}$ to $Sb^{5+}$. The presence of enough $As^{5+}$ can lead to the formation of $SbAsO_4$ which decreases the amount of antimony in solution by precipitation into the slimes (Kamath *et al.*, 2003; Braun, Rawling & Richards, 1976; Demaerel, 1987; Peng, Zheng & Chen, 2012; Wang *et al.*, 2010; Wang *et al.*, 2011). $SbAsO_4$ formation is of interest as it has been found in commercial slimes (Chen and Dutrizac, 1989; Chen & Dutrizac, 1991) but has been reported to be thermodynamically unstable above 60°C under electrorefining conditions (Wang *et al.*, 2006).

The lack of arsenic in the anode material, or an increase in Sb or Bi, corresponds to an increase in anode passivation, a decrease in current efficiency, and increase in nodule formation on the cathode (Kamath *et al.*, 2003; Moeller & Friedrich, 2010; Moats & Hiskey, 2006; Free & Anthian, 2000). Kamath *et al.* (2003) found that maintaining an anode arsenic content greater than 350 ppm prevented passivation, and that at least 300 ppm was required to prevent passivation of the anode when using a current density of 320 $A/m^2$ and electrolyte arsenic concentration of 12-15 g/L. Krusmark, Young & Faro

(1995) also reported that 300 ppm As was necessary to prevent passivation of the electrode.

Whether the mechanism is one of direct precipitation of impurity on the cathode or are carried to the cathode material, the cooler portions of the cathode have been shown to contain the predominance of impurities (Braun, Rawling & Richards, 1976). $Sb^{5+}$ creates 'floating slimes' of amorphous, Group-15 element compounds that cause entrainment of antimony and other elements into the cathode material (Braun, Rawling & Richards, 1976; Demaerel, 1987; Hiskey, 2012; Peng, Zheng & Chen, 2012; Wang *et al.*, 2006; Wang *et al.*, 2010; Wang *et al.*, 2011). Braun *et al.* (1976) also observed that floating slimes formed when total antimony concentrations exceeded 0.5 g/L. By maintaining lower concentrations of antimony in the electrolyte, floating slimes are avoided. Braun *et al.* (1976) further stated that the formation of floating slimes is due to undersaturation of Sb and Bi in the electrolyte with respect to the formation of antimony and bismuth arsenate. Saturation occurs when sufficient arsenic is added to increase the solubility product of [As] and [Sb] in the electrolyte above about 1.4 $g^2/L^2$. This first estimation does not take into account the activity of the species in solution.

Peng *et al.* (2012) reported that while As(V) is critical to the formation of falling slimes, and thereby the prevention of floating slimes, the activity of the As(V) compound in which it participates appears to have an effect on the formation of falling slimes. Peng *et al.* agreed with Wang *et al.* (2006) that both floating and falling slimes are of similar composition and consist of As/Sb-Ox, As/Sb-OH, and Sb-O(Y) compounds; where Y is a Group 15 element.

Wang *et al.* (2010) stated that at least 7 g/L of arsenic in the electrolyte is required to generate sufficient slime fall to reduce floating slime formation. These floating slimes compete with precipitating slimes for As, Sb, and Bi. It is also suggested by Wang *et al.* (2011) that the mole ratio of As(III)/As(V) is critical to the oxidation reaction of Sb(III) to Sb(V) and should be maintained < 0.09. It was further stated that the presence of Te and Se compounds can cause significant changes in this ratio (Wang *et al., 2011).* However, Demaerel (1987) indicated that an increase of As(III), independent of As(V), was used to prevent floating slimes.

The effects of glue, antimony, and chloride on copper deposit brittleness and structure were investigated using synthetic solutions (O'Keefe and Hurst, 1978). It was found that [Sb] > 300 ppm in the electrolyte produced brittle cathode material as determined by a simple bend test. These same cathodes were examined using Auger electron spectroscopy and found to contain greater amounts of antimony than more ductile cathode. They further found that the introduction of $Cl^-$ at levels between 1-5 ppm resulted in ductile cathode and a reduction in antimony found in the material. Deposits were roughened when chloride content matched or exceeded 15 ppm, but this effect was countered with the addition of glue to the electrolyte, producing smooth deposits.

The objective of this work is to replicate the reduction in starter sheet ductility in a laboratory setting that was observed in an industry setting (Wesstrom, 2014) and to evaluate possible underlying causes and mechanisms. The eventual goal would be to determine a more ecologically and economically viable solution than adjusting the anode molar ratio at the smelter.

## EXPERIMENTAL

## SOLUTION ANALYSIS

### ARSENIC AND ANTIMONY SPECIATION

Arsenic speciation was determined by the combination of titration and atomic absorption spectrometry (AAS). As (III) was determined by titration using bromate ion (Hangzhou University, 1984). A 5 mL aliquot of electrolyte was placed in a 250 mL Erlenmeyer flask. 20 mL of sulfuric acid was added, followed by 50 mL of distilled $H_2O$. To this hot solution, three drops of methyl orange indicator were added. The solution is immediately titrated while still hot (~60°C) with 3 g/L potassium bromate solution to a clear, intense-green endpoint. The resulting titrant volume is analyzed according to the reaction of Eq. 1.

$$3As^{3+} + BrO_3^- + 6H^+ \Leftrightarrow 3As^{5+} + Br^- + 3H_2O \qquad \text{Eq. (1)}$$

Antimony (III) was determined by a solvent extraction process using DDTC in chloroform as described by Noguchi *et al.* (1994). Aliquots of solution were placed in 250 mL separatory funnels to produce an aqueous to organic ratio (A:O) of 0.25. The organic portion consisted of a 400 mg/L solution of DDTC dissolved in chloroform. This extractant targets $Sb^{3+}$, leaving $Sb^{5+}$ in the aqueous solution. Using atomic absorption spectrometry (AAS), the concentrations of antimony in the aqueous solution were determined before and after solvent extraction. The before value was the total Sb concentration. The after value was the Sb (V) concentration. The difference was Sb (III).

**ELECTROREFINING CELL**

Samples of commercial anodes with molar As/(Sb+Bi) ratios of 0.54 and 3.8 were received from a copper refinery. Anode compositions as provided by the refinery are presented in Table 1. The anode samples were 7.62 x 17.78 x 5.08 cm cut from the original anode via waterjet. A used commercial titanium cathode was also provided in the same cut condition of dimensions 7.62 x 17.78 x 0.32 cm. Both the anode and cathode pieces were drilled for bolt holes placed 1.59 cm from each edge, and 1.27 cm from the top of the electrode such that the length of each would hang into the electrolyte leaving 5.08 cm of the electrode exposed above the solution line. Bus bars were fashioned from 2.54 x 0.32 cm copper bar that spanned the cell, from which each electrode hung, being affixed by 0.635 cm stainless steel bolts. The titanium cathode pieces were fitted with redundant edge strips consisting of vinyl tape, a rubber strip, and clear, dried acrylic nail polish to prevent plating on the edges. Eventually, the rubber strips decayed and were discarded, leaving the tape and polish, which were adequate. The edge strips extended approximately 0.32 cm from the edge onto the face of the cathode, around the perimeter, reducing the effective plating area and necessary current.

Table 1: Electrorefining Anode Assays

| Molar Ratio | Antimony Assay (ppm) | Bismuth Assay (ppm) | Arsenic Assay (ppm) | Nickel Assay (ppm) | Sulfur Assay (ppm) | Oxygen Assay (ppm) |
|---|---|---|---|---|---|---|
| 3.82 | 151 | 14 | 373 | 153 | 13 | 0.117 |
| 0.54 | 141 | 19.9 | 50.4 | 133 | -- | -- |

The laboratory cell consisted of a rectangular polypropylene (PP) container measuring approximately 35.56 x 25.4 x 25.4 cm. Slots were cut into the longest sides of the PP lip, into which the copper bus bars fit snugly to mitigate any movement of the electrodes. The cell was operated with three anodes and two cathodes. Cathode-to-cathode spacing is 11.3 cm. Holes were drilled in the PP on each of the shorter sides of the cell through which the electrolyte tubing would pass for circulation of the fluid. The ends of the inflow tubes were approximately 0.5 cm from the bottom of the cell. The electrodes were perpendicular to the electrolyte flow.

Standard battery clamps, wired to the EXTECH Instruments' adjustable switching mode power supply and attached to each bus bar, provided the necessary current. Current was maintained within ± 0.25 A among all of the electrodes as measured using an induction, clamp-on ammeter.

Two Briskheat® model SRP06241P, 180 watt silicon blanket heaters, designed for PP, were attached to the outside of the container, completely encompassing the perimeter. A layer of insulation was placed around these to reduce heat loss. Both heaters and a thermocouple were wired to a Digi-Sense TC5000 single-zone temp controller. The thermocouple was placed in the center of the cell, not in contact with any electrodes.

Electrolyte flow was approximately 25 mL/min through four (4) channels of a Cole-Parmer Masterflex L/S Economy Drive pump, using a Masterflex L/S multichannel pump head (model 7535-04) and Tygon E-Lab size L/S 14 tubing.

A Masterflex L/S model 7528-30 precision pump drive, using a Masterflex L/S multichannel pump head (model 7525-04) and Tygon E-Lab size L/S 13 tubing, was used for the addition of glue, avitone, and later thiourea over the course of the plating cycles.

Additives (glue, avitone, and thiourea) were prepared before each experimental series. 10 g glue was prepared in a 1 L volumetric flask. In a 500 mL volumetric flask, 5

g avitone was dissolved. Commercial glue, avitone, and thiourea were provided by a copper refinery.

## CELL OPERATION

The lab electrorefining cell was operated for a 21 hour plating cycle using 8.5 A (cathode current density = 265 $A/m^2$) and 65°C. The cell was brought to temperature a day in advance, with all electrolyte and electrodes present. The power supply was turned off within 10 minutes of 21 hours, consistently. A cycle was followed by stripping and cleaning of the cathodes, and replacement of the additives and water in a reservoir. Then another plating cycle was performed. 14 or 15 plating cycles were performed per condition or series. Three experimental series were run to determine the effect of anode composition and the addition of thiourea to the daily glue. Series 1 was run using anodes with a molar ratio 0.54; Series 2 used anodes with a molar ratio of 3.8; Series 3 used the lower molar ratio anode, and thiourea was added to the daily glue at a 1:1 weight ratio.

## ELECTROLYTE

30 gallons of stripper electrolyte was provided by a copper refinery. It was stored at room temperature after shipment. Solution assays indicate that the initial concentrations of copper, arsenic, and antimony were 49 g/L, 5.8 g/L, and 0.2 g/L, respectively.

## ADDITIVES

The setting of the additive pump varied slightly with alterations in evaporation rate due to atmospheric conditions, but was generally maintained at a flow rate of 2.2 to 2.3 mL/min (6.0 to 6.4 dial setting). 570 µL of avitone solution and 5.1 mL of glue solution, both of 10 g/L, were added via pipet to a reservoir of deionized, distilled water to be added over the course of the 21 hour plating cycle by the additive pump. This also had the effect of replacing fluid lost due to evaporation. Thiourea was later added in a 1:1 ratio with glue by the same mechanism as avitone and glue. Nominal total electrolyte volume was approximately 17.9 L, added after electrodes were hung in the cell, and leaving headspace of approximately 5.08 cm.

Top glue was added in 9 mL portions at 10 g/L between each of the electrodes for a total of 36 mL added. This was done within ten minutes before starting the plating cycle.

### STRIPPING AND CATHODE MAINTENANCE

At the end of each plating cycle, the cathodes were removed from their slots, rinsed with distilled, deionized water, and stripped by hand. The stripped copper was then placed in an ultrasonic distilled, deionized water bath for about 2 minutes.

The titanium cathode surfaces were never machined, abraded, or altered in any way from the as-received commercial state, except for the stated water rinse. Cathode edge strips of vinyl tape and acrylic polish were maintained as needed during the experiments. If excessive difficulty was had in stripping the cathode, or if the tape had begun wearing, it was replaced. Usually, this was necessary about every 2-3 days.

### SAMPLING

Before each experimental series, the new electrolyte was sampled. At the end of each 21 hour plating cycle, approximately 60 mL of electrolyte sample was taken evenly from around the cell using a plastic transfer pipet. These samples would be used to measure electrolyte composition.

### SERIES CHANGE

Each experimental series was entirely independent. The cell was drained and rinsed thoroughly, and the tubing was either thoroughly cleaned or replaced, if necessary. Both electrode and anode pieces were replaced for each series. Fresh electrolyte was used at the start of each series.

## PHYSICAL CHARACTERIZATION OF STARTER SHEETS

### BEND TEST

The ductility of the harvested lab cathode material was tested using a standard industrial bend test (Wesstrom, 2014). The material was placed lengthwise in a vice, grasped with a wide-jaw Vice-Grips® approximately 1.27 cm above the vice. The material is bent, evenly, at 90° in each direction. Each motion is counted as one bend.

The total number of bends for each sheet is recorded. Failure was determined by visual observation of a crack, or rumpling of the bend surface in more ductile material.

### XRD

XRD was performed using a PANalytical X'Pert Pro Multi-Purpose Diffractometer (MPD). Two cathodes from each experimental series had sections removed from them measuring approximately 1 $cm^2$ (0.16 $in^2$). A single measurement on the surface of each specimen was recorded, and the results for each series were averaged.

### MICROSCOPY

Cathode samples for optical microscopy were ground and polished to a mirror finish (0.03-0.05 μm colloidal silica). A standard potassium chromate etchant was applied under running water for 5-15 seconds. Etched samples were examined under reflected light. Dark field images were also acquired.

## RESULTS AND DISCUSSION

The purpose of this study was to examine the effects of anode composition and thiourea on the production of starter sheet material. Commercially, it has been noted that a higher As/(Sb+Bi) molar ratio in the anode resulted in more ductile starter sheets (Wesstrom, 2014). When the anode ratio was too low, the cathode quality suffered and starter sheet loop failures increased.

### BEND TEST

Samples of laboratory deposited starter sheets were evaluated for ductility using the bend test described in the experimental section. Each sample was also measured for thickness at the center of the deposit. The thickness data was used to normalize the number of bends to failure with the thickness of each sheet. The bend test data are shown in Figure 1. For each experimental series, they are ordered sequentially by plating cycle number. A summary of the average bends to failure is presented in Table 2.

The data demonstrates the effects of both a higher anode molar ratio and the addition of thiourea on increasing the number of bends to failure. Student's t-test was applied to these data and found the means of each data set were different with 95% confidence. The results of Series 1 and 2 appear to follow the expectation from

commercial reports. That is, the higher anode molar ratio increased the bend test numbers.

There is an observable trend of increasing bends with plating cycle for each series. This is supported by regression analysis, with correlation values of 0.67 and 0.65 for bend test versus plating cycle for Series 1 and 2. Series 3 regression analysis is less substantial, having a correlation of only 0.41. More investigation is needed to adequately explain the trend of increased ductility with operation time.

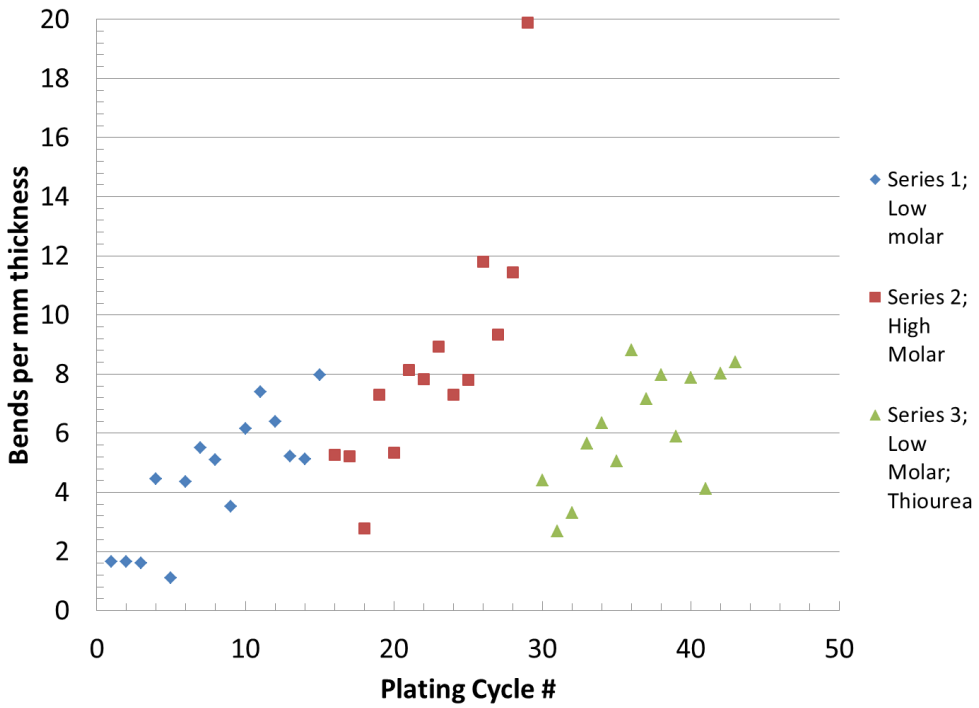


**Figure 1:** Number of bends to failure of each cathode normalized to the thickness versus plating cycle and series. The higher molar anode ratio increased the number of bends. The addition of thiourea likewise had a positive effect, although not as much.

**Table 2:** Summary of each series average bend test results and organic additives

| Series | **Anode As/(Sb+Bi) Molar Ratio** | **Daily Glue (g/tonne)*** | **Avitone (g/tonne)** | **Thiourea (g/tonne)** | **Average Bends Per mm Thickness** |
|---|---|---|---|---|---|
| 1 | 0.54 | 240 | 27 | 0 | 4 |
| 2 | 3.82 | 240 | 27 | 0 | 8 |
| 3 | 0.54 | 240 | 27 | 240 | 6 |

*-prior to each 21-hour plating cycle 1800 g/tonne of top glue was added to the electrolyte

## SOLUTION ANALYSIS

Each 21 hour plating cycle resulted in the collection of approximately 60 mL of electrolyte for chemical analysis of antimony and arsenic.

### ANTIMONY

$Sb^{5+}$ concentration data versus plating cycle and series are presented in Figure 2. The significantly lower concentration of $Sb^{5+}$ in Series 2 is particularly notable. Total antimony and $Sb^{3+}$ concentrations are presented in Figure 3. A summary of the antimony data is presented in Table 3.

A statistical analysis of the data, using Student's t-test, confirms that there is significant difference among all three data sets to a 95% confidence level for both total antimony and $Sb^{5+}$. $Sb^{3+}$ results are indistinguishable between series 1 and 3, indicating that the addition of thiourea had no statistically significant effect on $Sb^{3+}$ concentration. These observations indicate that anode molar ratio and thiourea addition each had a significant observable effect on the valence and total concentration of antimony in solution.

There appears to be a decrease in $Sb^{5+}$ over the course of the experiments in series 1 and 3. Any decrease that may be present in series 2 was undetectable. These trends are not understood and would require further investigation.

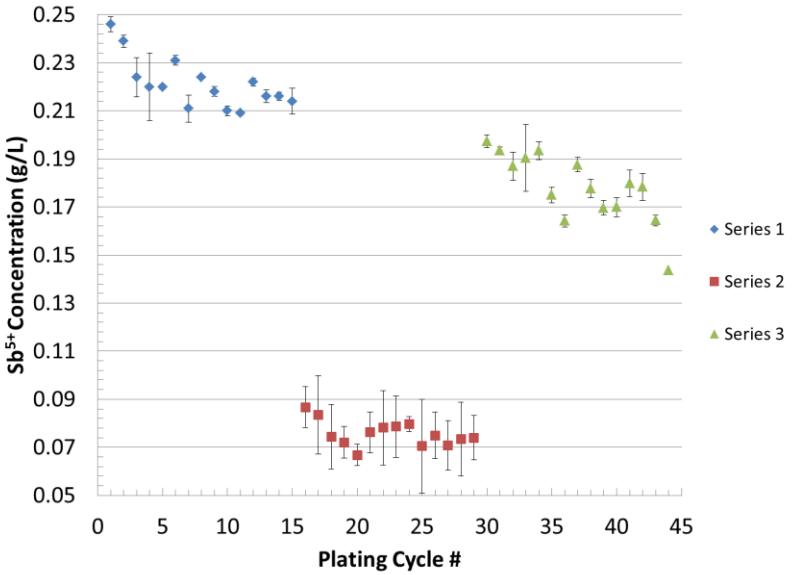


**Figure 2:** Sb(V) concentration versus plating cycle and series. A noted drop in antimony (V) occurs in Series 2, when using a higher molar ratio anode. Error bars indicate 95% CI on valence analysis.

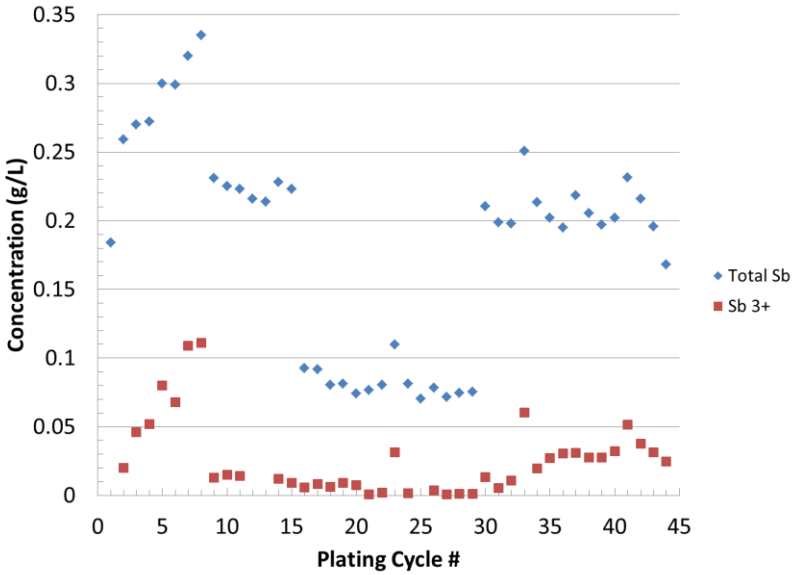


**Figure 3:** Total antimony and $Sb^{3+}$ concentrations versus plating cycle.

The electrolyte data clearly indicates that high molar ratio anodes reduce the concentrations of $Sb^{5+}$ and total Sb in the electrolyte. It is assumed that the antimony has

reported to the anode slimes. Unfortunately, the quantity of slimes produced from these anodes was limited and chemical analysis of the slimes was not performed.

The thiourea appears to act as a reducing agent for antimony in solution. More Sb was found as $Sb^{3+}$ in the presence of thiourea than in its absence. It is suspected that thiourea oxidizes to formamidine disulfide thus, reducing $Sb^{5+}$ to $Sb^{3+}$. However, the exact mechanism is likely much more complex since thiourea is also known to oxidize in the presence of cupric ion and form complexes with cuprous ions.

Table 3: Summary of each series average antimony and arsenic concentrations

| **Series** | **Condition** | **Sb (g/L)** | **$Sb^{3+}$ (g/L)** | **$Sb^{5+}$ (g/L)** | **As (g/L)** | **$As^{3+}$ (g/L)** | **$As^{5+}$ (g/L)** |
|---|---|---|---|---|---|---|---|
| 1 | 0.54 Anode Molar Ratio, No Thiourea | 0.25 | 0.03 | 0.22 | 5.1 | 1.1 | 4 |
| 2 | 3.82 Anode Molar Ratio, No Thiourea | 0.081 | 0.006 | 0.076 | 5.3 | 0.76 | 4.6 |
| 3 | 0.54 Anode Molar Ratio, Thiourea Added | 0.21 | 0.03 | 0.18 | 5.4 | 0.89 | 4.5 |

Figure 4 shows a strong correlation between the drop in antimony valence concentrations and the increase in bend test results. Thus, it appears that $Sb^{5+}$ concentration in the electrolyte is linked to the mechanical performance of the cathode material.

**ARSENIC**

Arsenic concentrations in the electrolyte were reasonably stable between 5-6 g/L through all of the plating cycles. Most arsenic occurred as $As^{5+}$ [83% of As was $As^{5+}$ on average], as would be expected if the oxidation of arsenic precedes the oxidation of antimony. Figure 5 demonstrates the concentrations of arsenic and its valence states in the electrolyte over the course of all three experimental series. A summary of the arsenic data is presented in Table 3.

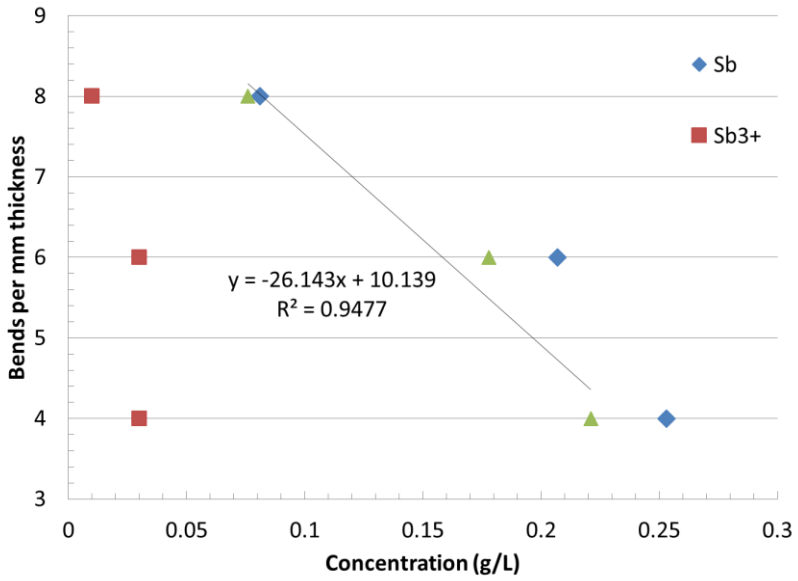


**Figure 4:** Correlation between the concentration of antimony (V) and bend test results.

Student's t-test was applied to all arsenic data sets to determine if any significant differences could be quantified. Series 1 & 3 displayed a statistically significant difference with a 95% CI for both total arsenic and $As^{5+}$ concentration. Each series was different in terms of $As^{3+}$ concentration at 95% confidence. This is more easily observed in Figure 6. Thus, it would seem to follow that the series with more desirable bend test results contained a lower proportion of $As^{3+}$ than the other two series. The third series, using thiourea, has a somewhat higher concentration of $As^{3+}$, but still lower than the first series when no thiourea was added.

Further, there appears to be a strong correlation between decreasing As (III) concentration and increasing bend test results as shown in Figure 7. There was no apparent correlation between the As(III)/As(V) molar ratio and the number of bends to failure exhibited by each cathode.

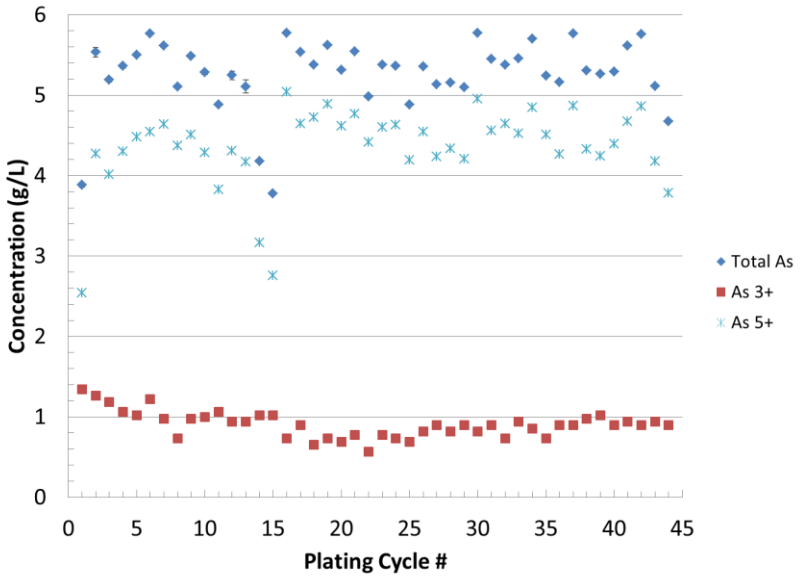


**Figure 5:** Concentration of arsenic and its valence states versus plating cycle.

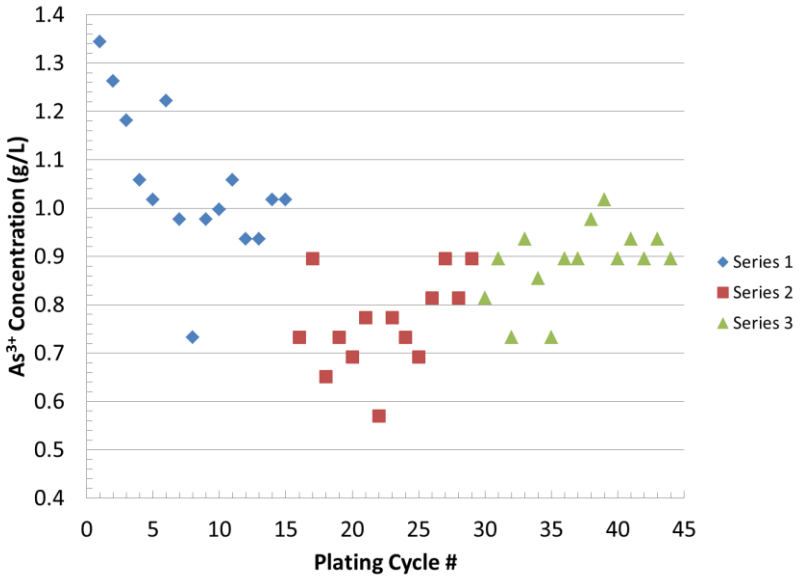


**Figure 6:** Concentration of $As^{3+}$ versus plating cycle and series.

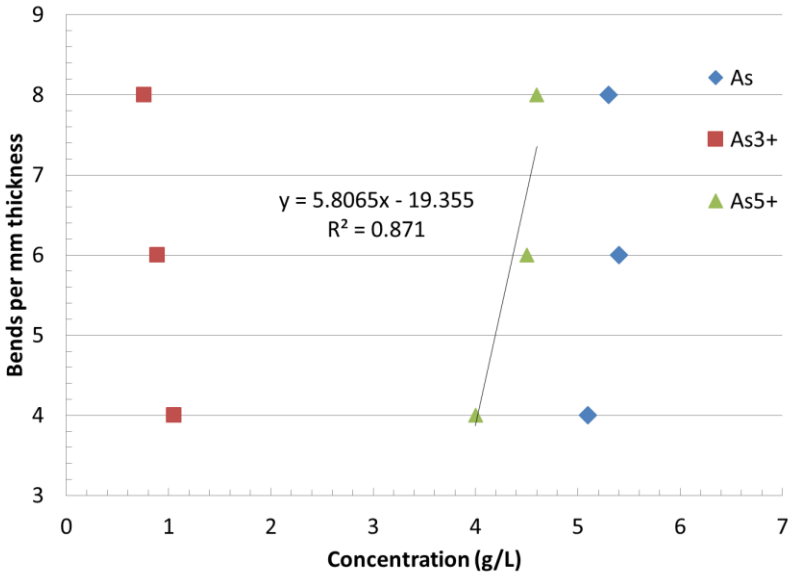


**Figure 7**: Correlation between rising $As^{5+}$ valence concentrations

## CATHODE CROSS SECTIONS

Micrographs of cathode samples from each experiment series were prepared according to standard metallography procedures to a final polish of 0.05 µm. Example micrographs are presented in Figure 8(a-d). While many of the specimens displayed a columnar grain structure, some did not. There did not appear to be a consistent pattern with respect to which sample showed equiaxed structures. No correlation was made between the cross-section microstructure and ductility results.

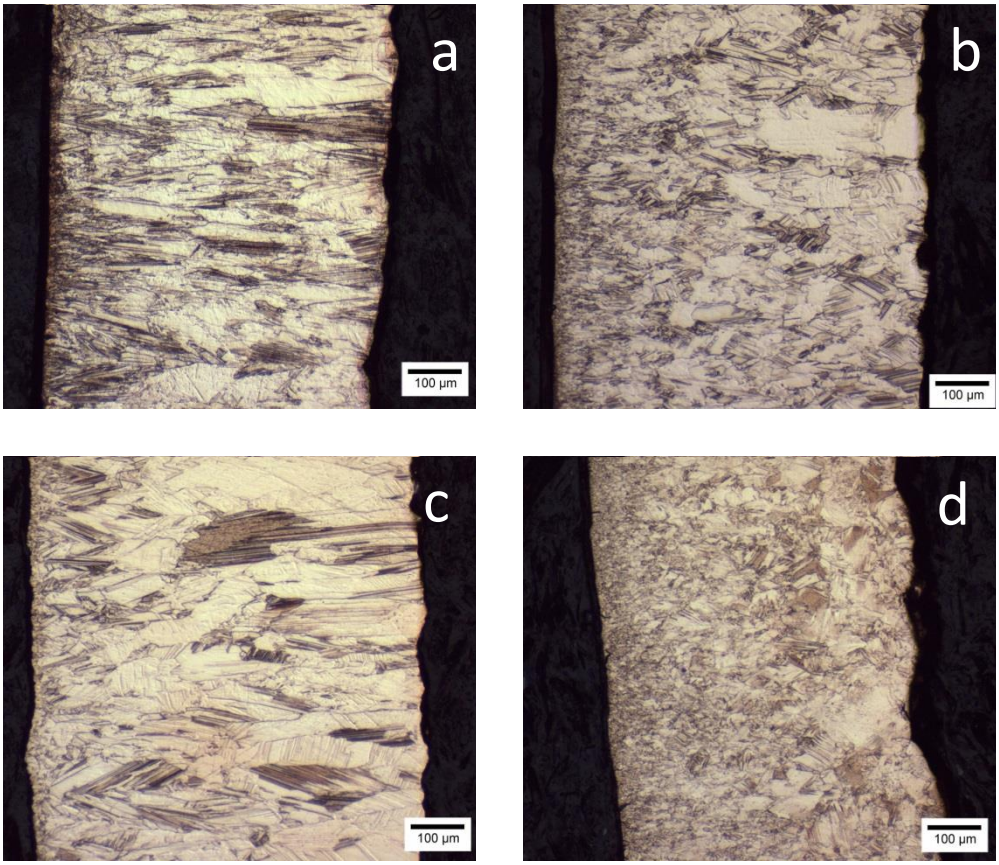


**Figure 8(a-d):** Cross section micrographs of cathode material. Series 1 (a,b) samples showed largely columnar grain structure, as in Series 2 (c), though the latter is more pronounced. The example for Series 3 (d) displays a more equiaxed grain structure. Substrate surface is located on the left of each image. Etched with potassium chromate.

**XRD ANALYSIS**

Analysis of the top surface with XRD instrumentation was completed on two cathode samples from each series. Figure 9 shows examples of the XRD patterns yielded from a cathode of each experimental series. Series 1 shows a strong (220) orientation with no observable (111) or (200) growth. Series 2 demonstrates the strongest growth of the (111) and (200) planes, corresponding to the higher molar ratio anode. The addition of thiourea in Series 3 generated some growth in the (111) and (200) planes, but not as much as that seen in Series 2. Figure 10(a,b) highlight the increased presence the (111) and (200) planes for the experiments run with higher molar ratio anodes (Series 2) and thiourea addition (Series 3). The increasing presences of (111) and (200) planes correlate with increasing bends in the bend test as shown in Figure 11.

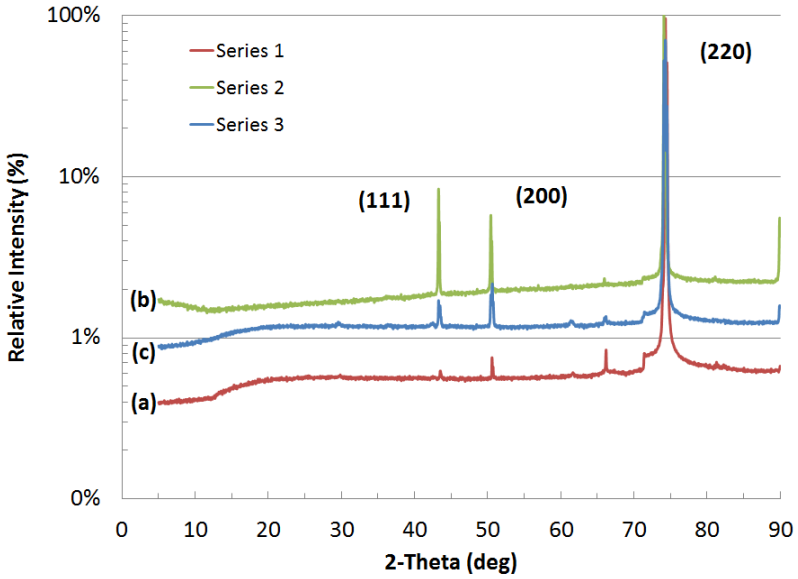


**Figure 9:** Examples of XRD patterns from each experimental series. Lower molar ratio anode without thiourea (a) resulted in a predominantly (220) oriented structure, while the use of higher molar ratio anode (b) had growth in the (111) and (200) planes. The addition of thiourea to the lower molar ratio anode (c) resulted in some mixed-grain character of (111) and (200), but less than Series 2.

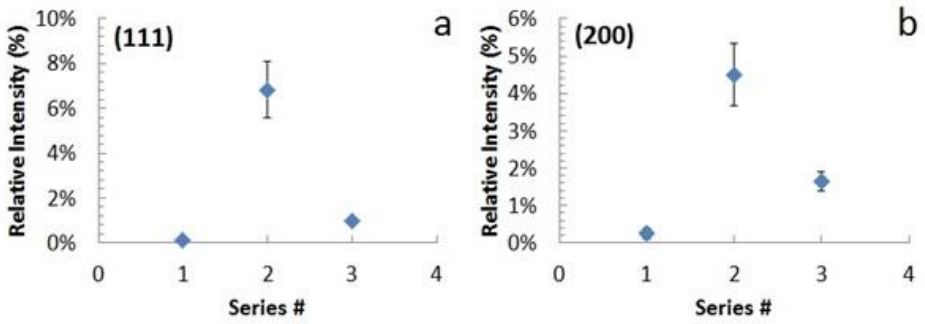


**Figure 10 (a,b):** XRD intensities of (111) and (200) planes on the surface of cathode material according to series**.**

The presence of other crystallographic planes parallel to the cathode surface indicates a more mixed-grain structure for Series 2 and 3. This is a likely source for the increased ductility observed in the bend test. A more isotropic material typically performs better during physical testing due to more uniform inhibition of dislocation movement throughout the material.

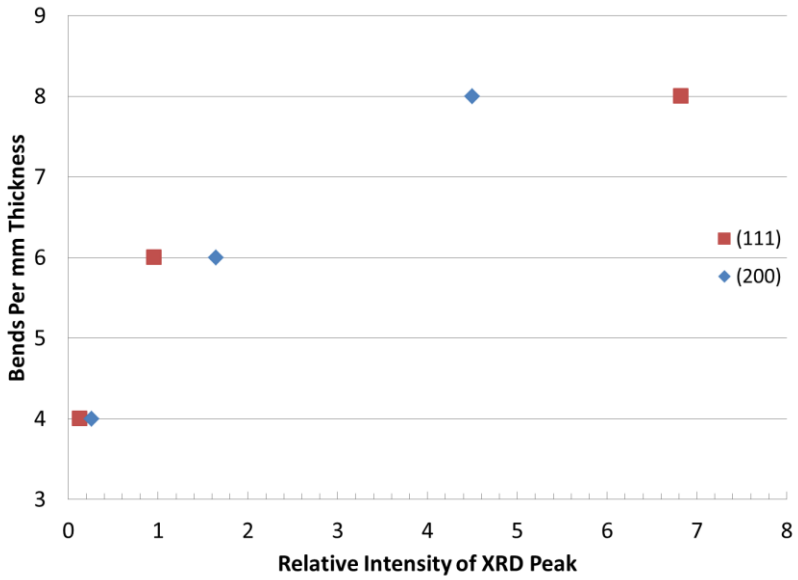


**Figure 11**: Bend test results versus relative intensity of (111) and (200) planes determined by XRD.

## CONCLUSIONS

It is evident from the experimental data that there is a significant effect from the initial anode composition on the physical properties of the cathode material produced as copper starter sheets by electrorefining. The average bend test results for the higher molar ratio anode were 100% better than the lower molar ratio anode was used (8 bends per mm vs. 4).

The addition of thiourea to the electrolyte also had a statistically and visually observable effect on the cathode ductility, increasing the bend test results by 50% on average when the lower molar ratio anode was used.

The mechanism of the improved ductility is believed to be caused by a more mixed grain structure (e.g. the increasing presence of (111) and (200) growth). The presence of other crystallographic planes appears to improve the ductility of the starter sheets.

Electrolyte chemistry has a strong effect on cathode ductility, as well. Electrolytes with lower Sb, $Sb^{5+}$ and $As^{3+}$ correlated with improved ductility. There appears to be no correlation between quality cathode production and As(III)/As(V) molar ratio. It appears that anode molar ratio and thiourea addition are also modifying the

electrolyte chemistry. The mechanism by which electrolyte chemistry affects deposit ductility still needs to be determined.

**REFERENCES**

Baltazar V., Claessens P.L., Thiriar J. (1987) "Effect of arsenic and antimony in copper electrorefining", *The Electrorefining and Winning of Copper*, Eds. J.E. Hoffmann, R.G. Bautista, V.A. Ettel, V. Kudryk and R.J. Wesely, TMS, Warrendale, PA, U.S.A., pp. 173-195.

Braun T.B., Rawling J.R., Richards K.J. (1976) "Factors affecting the quality of electrorefined cathode copper", *International Symposium on Copper Extraction & Refining*, Las Vegas, Nevada, pp. 511-524.

Chemistry Department (1984), Hangzhou University; *Chemical Analysis (Analytical Chemistry Handbook, Part II)*; Chemical Industry Press, Beijing (in Chinese).

Chen, T. T., and J. E. Dutrizac. (1989), "Mineralogical Characterization of Anode Slimes—IV. Copper-Nickel-Antimony Oxide ("Kupferglimmer") in CCR Anodes and Anode Slimes." *Canadian Metallurgical Quarterly* 28.2, pp. 127-134.

Chen, T. T., and J. E. Dutrizac. (1991), "Mineralogical Characterization of Anode Slimes: Part 7—Copper Anodes and Anode Slimes From the Chuquicamata Division of Codelco–Chile." *Canadian metallurgical quarterly* 30.2, pp. 95-106.

Demaerel J.P. (1987) "The behavior of arsenic in the copper electrorefining process", *The Electrorefining and Winning of Copper*, Eds. J.E. Hoffmann, R.G. Bautista, V.A. Ettel, V. Kudryk and R.J. Wesely, TMS, Warrendale, PA, U.S.A., 195-210.

M.L. Free and L. Anthian, (2000), "The effect of anode impurities on copper electrorefining", *SME Preprint 00-62*, Littleton, CO, U.S.A.

Hiskey J.B. (2012) "Mechanism and Thermodynamics of Floating Slimes Formation", *T.T. Chen Honorary Symposium on Hydrometallurgy, Electrometallurgy and Materials Characterization,* pp. 101-112.

Kamath B. P., Mitra A.K., Radhakrishnan S., Shetty K.P., (2003) "Electrolyte impurity control at Chinchpada Refinery of Sterlite Industries (India) Limited", *Copper Electrorefining and Electrowinning*, pp. 137-150.

Krusmark T.F., Young S.K., and Faro J.L. (1995) "Impact of anode chemistry on high current density operation at Magma Copper's electrolytic refinery", *In Copper 1995, W.C. Cooper, D.B. Dreisinger, J.E. Dutrizac, H. Hein and G. Ugarte, Eds., Canadian Institute of Mining, Metallurgy and Petroleum, Montreal, Canada*, vol. 3, pp. 189-206.

Möller C.A.., Friedrich B., (2010) "Effect of As, Sb, Bi and Oxygen in Copper Anodes During Electrorefining." *Proceedings of Copper*.

Noguchi F., Yano M., Nakamura T., Ueda Y. (1994) "Form of Antimony Dissolved into Electrolyte During Copper Electrorefining", *Metallurgical Review of MMIJ*, vol. 11, pp. 38-52.

Noguchi F., Itoh H. and Nakamura T., (1995) "Effect of impurities on the quality of electrorefined cathode copper, behavior of antimony in the anode" *In Copper 1995, W.C. Cooper, D.B. Dreisinger, J.E. Dutrizac, H. Hein and G. Ugarte, Eds., Canadian Institute of Mining, Metallurgy and Petroleum, Montreal*, Canada, vol. 3, pp. 337-348.

O'Keefe T. J., Hurst L. R. (1978) "The effect of antimony, chloride ion, and glue on copper electrorefining", *Journal of Applied Electrochemistry*, vol 8, pp. 109-119.

Peng, Y., Zheng Y., and Chen W. (2012), "The oxidation of arsenic from As (III) to As (V) during copper electrorefining." *Hydrometallurgy* 129, pp. 156-160.

Wang, X., Chen Q., Zhou-Lan Y., Lian-Sheng X. (2006), "Identification of arsenato antimonates in copper anode slimes", *Hydrometallurgy*, 84, pp. 211–217.

Wang, X., Chen Q., Zhou-Lan Y., Wang M., Xiao B., Zhang F., (2010) "Homogeneous precipitation of As, Sb and Bi impurities in copper electrolyte during electrorefining", *Hydrometallurgy*, 105, pp. 355-358.

Wang X., Chen Q., Zhou-Lan Y., Wang M., Xiao B., Tang F., (2011) "The role of arsenic in the homogeneous precipitation of As, Sb, and Bi impurities in copper electrolyte", *Hydrometallurgy*, 108, pp. 199-204.

Wenzl C. (2008), "Structure and casting technology of anodes in copper metallurgy", *Dissertation. Montanuniversität Leoben, Leoben, Austria.*

Wesstrom B. (2014) "The Effects of High Antimony in Electrolyte", *COM 2014-Conference of Metallurgists Proceedings ISBN:978-1-926872-24-7.*

# SECTION

# 3. CONCLUSIONS

The work performed for copper electrowinning was able to replicate the problems seen in industry due to manganese (II) coming through the hydrometallurgical process, and the application of a commercial polyacrylamide was observed to significantly reduce the passivation of a coated titanium anode. Other organic additives did not demonstrate any effect on the anode passivation.

Industrial results using lower molar ratio [As/(Sb+Bi] copper cathode were replicated using a laboratory cell, appropriately scaled down from a commercial copper electrorefining, stripper cell. The poor ductility of cathode was remedied by a change in anode chemistry to higher molar ratio. The addition of the organic thiourea in a 1:1 mast ratio with the continuous, process glue exhibited an increase in cathode ductility, but not as extreme as the change in anode chemistry alone.

# VITA

Paul Laforest was born AD1990 in the Midwest United States. He graduated from Lutheran High School South in Affton, MO in 2009. He continued his education at Missouri University of Science and Technology where he earned a B.S. in Metallurgical Engineering and began his graduate studies in June 2014 under Dr. Michael Moats. He received his M.S. in Metallurgical Engineering in December of 2015.